Particular features of ternary fission induced by polarized neutrons in the major actinides ^{233,235}U and ^{239,241}Pu

A. Gagarski,[1,*] F. Gönnenwein,[2] I. Guseva,[1] P. Jesinger,[2] Yu. Kopatch,[3] T. Kuzmina,[4] E. Lelièvre-Berna,[5] M. Mutterer,[6,7] V. Nesvizhevsky,[5] G. Petrov,[1] T. Soldner,[5] G. Tiourine,[8] W. H. Trzaska,[8] and T. Zavarukhina[1]

[1]*Petersburg Nuclear Physics Institute of National Research Centre "Kurchatov Institute," 188300 Gatchina, Russia*
[2]*Physikalisches Institut, Universität Tübingen, D-72076 Tübingen, Germany*
[3]*Frank Laboratory of Neutron Physics, Joint Institute for Nuclear Research, 141980 Dubna, Russia*
[4]*Khlopin Radium Institute, 194021 St. Petersburg, Russia*
[5]*Institut Laue-Langevin, F-38042 Grenoble, France*
[6]*Institut für Kernphysik, Technische Universität Darmstadt, D-64289 Darmstadt, Germany*
[7]*GSI Helmholtzzentrum für Schwerionenforschung GmbH, D-64291 Darmstadt, Germany*
[8]*Department of Physics, University of Jyväskylä, FIN-40014 Jyväskylä, Finland*

(Received 23 June 2015; published 24 May 2016)

Ternary fission in (n,f) reactions was studied with polarized neutrons for the isotopes ^{233,235}U and ^{239,241}Pu. A cold longitudinally polarized neutron beam was available at the High Flux Reactor of the Institut Laue-Langevin in Grenoble, France. The beam was hitting the fissile targets mounted at the center of a reaction chamber. Detectors for fission fragments and ternary particles were installed in a plane perpendicular to the beam. In earlier work it was discovered that the angular correlations between neutron spin and the momenta of fragments and ternary particles were very different for ^{233}U or ^{235}U. These correlations could now be shown to be simultaneously present in all of the above major actinides though with different weights. For one of the correlations it was observed that up to scission the compound nucleus is rotating with the axis of rotation parallel to the neutron beam polarization. Entrained by the fragments also the trajectories of ternary particles are turned away albeit by a smaller angle. The difference in turning angles becomes observable upon reversing the sense of rotation by flipping neutron spin. All turning angles are smaller than 1°. The phenomenon was called the ROT effect. As a distinct second phenomenon it was found that for fission induced by polarized neutrons an asymmetry in the emission probability of ternary particles relative to a plane formed by fragment momentum and neutron spin appears. The asymmetry is attributed to the Coriolis force present in the nucleus while it is rotating up to scission. The size of the asymmetry is typically 10^{-3}. This asymmetry was termed the TRI effect. The interpretation of both effects is based on the transition state model. Both effects are shown to be steered by the properties of the collective (J,K) transition states which are specific for any of the reactions studied. The study of asymmetries of ternary particle emission in fission induced by slow polarized neutrons provides a new method for the spectroscopy of transition states (J,K) near the fission barrier. Implications of collective rotation on fragment angular momenta are discussed.

DOI: 10.1103/PhysRevC.93.054619

I. INTRODUCTION

The study of nuclear fission in (n,f) reactions with aligned or polarized targets and polarized neutrons as projectiles has highlighted particular features of the process. These studies were performed at accelerator driven pulsed neutron sources for neutrons in the resonance region and in the high neutron flux of nuclear reactors with energies albeit limited to a narrow range near the thermal point. Angular distributions of fragments from fission of oriented nuclei served to determine (J,K) quantum numbers of transition states at the saddle point for individual resonances of the cross section in ^{235}U(n,f) [1]. For the same reaction spin-dependent fission cross sections were obtained in a study of polarized ^{235}U targets irradiated by polarized neutrons [2].

A new line of research was opened with the discovery of parity violation in fission reactions [3]. In these experiments fragments were registered parallel and antiparallel to neutron spin $\boldsymbol{\sigma}_n$. Parity non-conservation (PNC) is disclosed by an asymmetry in the fragment angular distribution depending on the pseudoscalar product $(\boldsymbol{\sigma}_n \cdot \mathbf{p}_{\mathrm{LF}})$ with the light fragment momentum $\mathbf{p}_{\mathrm{LF}}$ being chosen for reference. With an observed asymmetry near 10^{-4} in the reaction ^{235}U(n,f) the size of the PNC effect is surprisingly large. This is because of the mixing of $s_{1/2}$ and $p_{1/2}$ states near p-wave resonances which otherwise are not visible.

With the exceptionally large polarized neutron fluxes at the High Flux Reactor of the Institut Laue-Langevin in Grenoble, France, it became possible to investigate even ternary fission in (n,f) reactions with polarized neutrons. With the ratio ternary/binary fission amounting to $t/b \approx 2 \times 10^{-3}$ ternary fission is a rare process. By far in most cases the ternary particle (TP) is an α particle. A remarkable result was the virtual equality of the PNC effect for fragments from both binary and ternary fission [4–6]. Because according to A. Bohr's theory of fragment angular distributions these are settled at the saddle point of fission, the PNC result indicates that binary and ternary fission share the same saddle point or, stated otherwise, the ternary particles are not foreshadowed at the saddle. Ternary particles come into being only at scission.

*gagarski@pnpi.spb.ru

Encouraged by the success to observe the violation of fundamental laws of physics like PNC in fission, the idea was ventured whether not also time reversal invariance could be tested [7]. In analogy to the search for violation of time reversal invariance in the decay of free polarized neutrons a triple correlation has to be analyzed between neutron spin $\boldsymbol{\sigma}_n$ and the momenta of fragments $\mathbf{p}_{\mathrm{LF}}$ and ternary particles $\mathbf{p}_{\mathrm{TP}}$. An experimental program covering several years has for the present come to a stage allowing reviewing new facets of fission phenomena albeit not related to time reversal invariance.

Ternary fission experiments induced by polarized neutrons for four fissile isotopes ^{233,235}U and ^{239,241}Pu are described in the following. The hope to find violation of time reversal invariance was not fulfilled. Instead two distinct phenomena could be scrutinized which were discovered earlier either in $^{235}\mathrm{U}(n,f)$ or $^{233}\mathrm{U}(n,f)$ reactions called ROT or TRI effect, respectively [8,9]. The ROT effect is attributed to be the collective rotation of the compound nucleus down to scission. The TRI effect reflects the influence of the rotating nucleus on the emission probability of ternary particles. Both effects are now shown to be present in parallel with different weights for all actinides studied. The results are discussed in terms of models focusing on the (J,K) properties of saddle transition states.

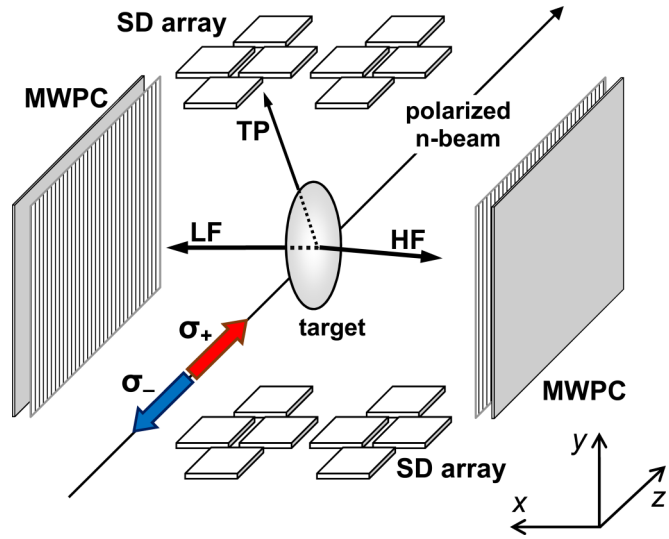

FIG. 1. Layout of the experimental setup. Fissile target at the center, polarized neutron beam running horizontally, two MWPC detecting complementary fission fragments to the left and right of target, two arrays of Si detectors on top and bottom of target intercepting ternary particles. All centers of particle detector assemblies lie in a plane perpendicular to the beam.

II. EXPERIMENTAL LAYOUT

The layout of experiments was motivated by the search for violation of time reversal invariance. In speculative analogy to free neutron decay an experiment was proposed [7] to explore the triple correlation B:

$$B = \boldsymbol{\sigma}_n \cdot (\mathbf{p}_{\mathrm{LF}} \times \mathbf{p}_{\mathrm{TP}}) = \mathbf{p}_{\mathrm{TP}} \cdot (\boldsymbol{\sigma}_n \times \mathbf{p}_{\mathrm{LF}}), \qquad (1)$$

with B the correlation function between neutron spin $\boldsymbol{\sigma}_n$ and the momenta $\mathbf{p}_{\mathrm{LF}}$ and $\mathbf{p}_{\mathrm{TP}}$ of the light fragment LF and the ternary particle TP, respectively. All vectors are understood to be unit vectors. The correlation changes sign under time reversal, i.e., it is T-odd. In case a $B \neq 0$ is found it may indicate a violation of time reversal invariance. However, at variance with PNC where a nonzero P-odd observable proves the violation of parity, a nonvanishing T-odd observable is only a necessary but not sufficient condition for violation of time reversal invariance.

The correlation B becomes maximal when all three vectors in Eq. (1) are orthogonal to each other. For the two particle momenta this condition is somewhat closely fulfilled by nature because the TPs are ejected from the neck between the two main fragments and the Coulomb forces focus the TP roughly perpendicular to the fission axis. The neutron spin then has to be oriented perpendicular to the plane spanned by the particle momenta. This is achieved in experiment by detecting fragments and ternary particles in a plane perpendicular to neutron beam polarization.

For the experiments polarized neutron beams from the instruments PF1B [10,11] and D3 [12] of the High Flux Reactor of the Institut Laue-Langevin in Grenoble, France were available. The layout of the experimental setup is sketched in Fig. 1. A fissile target is mounted at the center of a reaction chamber. The neutron beam is running horizontally in the z direction with its polarization chosen to be longitudinal. Particle detectors are mounted with their centers lying in the (x,y) plane running through the target perpendicular to the beam. Two multiwire proportional counters (MWPC) facing each other to the left and right of the target intercept fission fragments. Ternary particles are measured by two arrays of up to 12 Si detectors on the top and bottom of the target. A series of experiments was conducted with the uranium isotopes ^{233}U and ^{235}U, and the plutonium isotopes ^{239}Pu and ^{241}Pu. In all experiments typical count rates were $\sim 10^6$/s for binary fission and $\sim 10^2$/s for ternary fission. More in detail, on PF1B the collimated cold polarized neutron beam had an equivalent thermal flux of $\sim 10^9$ /(s cm^2), an energy of 4.5 meV, and a polarization of $(92 \div 95)\%$.

The neutrons were polarized longitudinally along the beam (see Fig. 1) by a multislit supermirror polarizer. The fissile targets at the center of the reaction chamber were oriented nearly parallel to the beam axis. For the U targets UF_4 was evaporated as a thin layer of $\sim 100\,\mu$g/cm^2 on a thin Ti foil ($\sim 100\,\mu$g/cm^2) transparent to fission fragments. The diameter of the active spot was ~ 8 cm. The total amount of fissile material was ~ 5 mg for ^{233}U and ^{235}U. For the Pu targets both sides of an aluminum foil with rectangular size (2×7 cm^2) and thickness $\sim 20\,\mu$m were covered with Pu oxide. On each side the total amount of Pu was ~ 1 mg. The aluminum backing was transparent for TPs but not for FFs. Unavoidably, the backing entailed a low energy cutoff for the TPs. The TP energies were corrected in the evaluation. The two position-sensitive MWPCs for registration of FFs were mounted at a distance of ~ 12 cm to the left and right from the target plane (see Fig. 1). The MWPCs with size 14×14 cm^2 were operated at low gas pressure. To that purpose

the reaction chamber (volume 40 liters) was filled with CF_4 as the counting gas at a pressure of 10 mbar. The signals from the MWPCs served as the stop for the measurement of FF time of flight.

For the registration of TPs two arrays of Si detectors were installed at a distance of ∼12 cm from the target on the top and bottom (see Fig. 1). The centers of the diode arrays and the MWPCs are at right angles to each other. The diodes had to be covered by a 25-μm aluminum foil to prevent their damage by FFs. The typical size of diodes was $3 \times 3\,\mathrm{cm}^2$. The number of diodes per array varied from 4 to 12 in the different experiments. For the ^{233}U target the TPs entered the diodes from the back side which allowed separating He and H isotopes by pulse-shape discrimination [13]. For all other reactions there was no specific TP identification. It should be recalled, however, that more than 90% of all TPs are α particles.

A minimum request for the characterization of fragments is the distinct identification of the light and heavy fragment group. For thin U targets on transparent backings masses of complementary FFs are conventionally determined by measuring the time of flights for complementary fragments. Time marks for start were obtained from the TP detectors and for stop from the MWPCs. The start signal had to be corrected for the flight time of TPs from the target to the detectors. The TP velocity was thereby calculated from the measured TP energy. The location of a fission event on the target is determined quite accurately from the position coordinates of complementary FFs on the two MWPCs which allow reconstructing the fission axis. The full width at half maximum (FWHM) of time-of-flight resolution was 1–2 ns.

In the off-line analysis the angles between TP and FF momentum vectors are calculated event-by-event. In particular the angle $\theta_{\mathrm{TP-LF}}$ between the ternary particle TP and the light fragment LF serving as reference is determined. Because of the extended size of the TP detectors the angular resolution is not better than 10–15°. The data are sorted according to kinetic energies E_{TP} of TPs and FFs masses M_{LF}. The estimated resolution for FF mass is ∼8 u as derived from the time resolution.

In the experiments with Pu targets on backings nontransparent to fragments the data are less detailed. Only one of the two complementary fragments can be observed. Its time of flight is determined from the corrected TP start signal and the stop signal from the MWPC. It has thereby to be assumed that fission fragments proceed from the center of the target. There is no mass resolution but the crucial distinction between LF and HF is satisfactory. Also the resolution for the angle $\theta_{\mathrm{TP-LF}}$ is worse than for the U targets. To minimize the loss in angular resolution for angles of interest around the axis of polarization the shapes of the targets were chosen to be rectangular $2 \times 7\,\mathrm{cm}^2$. The targets were positioned in the chamber of Fig. 1 with the longer side horizontally. The angular resolution achieved is considered to be sufficient for the present purposes.

The correlator B in Eq. (1) changes sign upon flipping the neutron spin $\boldsymbol{\sigma}_n$. The effects to be expected are small; it is therefore imperative to apply the spin flip technique. In the spin flip technique the neutron spin is periodically switched between parallel and antiparallel to the beam. Controlled by a quartz clock the spin was flipped periodically with a frequency near 1 Hz. In the treatment of data the difference in LF-TP coincidence count rates for the two spin orientations is evaluated. The difference is only sensitive to the spin-dependent part of the angular distributions of particles.

In formulas the suggested angular correlation between the momenta of fragments and ternary particles reads

$$W(\mathbf{p}_{\mathrm{LF}}, \mathbf{p}_{\mathrm{TP}}) d\Omega_{\mathrm{LF}} d\Omega_{\mathrm{TP}} \sim (1 + CB) W_0(\mathbf{p}_{\mathrm{LF}}, \mathbf{p}_{\mathrm{TP}}) d\Omega_{\mathrm{LF}} d\Omega_{\mathrm{TP}}, \quad (2)$$

with $W_0(\mathbf{p}_{\mathrm{LF}}, \mathbf{p}_{\mathrm{TP}})$ the basic correlation independent of spin of the neutron inducing fission. The well-known anisotropic emission of ternary particles with preference perpendicular to the fission axis is described by the basic distribution W_0. For polarized neutrons an additional asymmetry appears described by CBW_0. The size C of the correlation B is found by evaluating asymmetries A as the difference in number of coincidences for the two spin orientations normalized to the sum:

$$A = (N_\uparrow - N_\downarrow)/(N_\uparrow + N_\downarrow), \quad (3)$$

with $N_\uparrow$ and $N_\downarrow$ the number of counts for neutron spin parallel and antiparallel to the beam direction, respectively. Asymmetries A are evaluated for coincidences of ternary particles with fission fragments. By convention the sign of the asymmetry A quoted is the sign for the reference combination with the light fragment LF flying in Fig. 1 in the $+x$ direction and the ternary particle TP upwards with $y > 0$.

While measuring small physical effects by the technique of neutron spin flip, it is crucial to control and suppress spurious systematic asymmetries in experiment. In all our experiments the period of spin flip was chosen to be short (4 s maximum) thereby suppressing strongly false effects related to slow drifts of neutron flux, electronic channels, etc. The flipping times were controlled by a stabilized quartz clock with instability $< \pm 2\,\mathrm{ppm/°C}$ in the temperature range 0 °C–50 °C.

The symmetric arrangement of detectors shown in Fig. 1 further allowed measuring simultaneously asymmetries in the angular correlations between ternary particle and light fragment in four different geometries: up-left, up-right, down-left, and down-right. For a genuine spin-dependent effect all four asymmetries should be equal in absolute value but have proper sign correlations. Within statistical accuracy this was indeed observed. The four asymmetries were averaged with proper signs and quoted for the reference combination with the light fragment LF flying in Fig. 1 in the $+x$ direction and the ternary particle TP in the $+y$ direction. By contrast, when averaging with signs taken at face value the asymmetry was zero within statistical error. This proves that systematic effects are significantly smaller than the statistical uncertainties.

As a further way to assess false asymmetries, measurements were performed for two opposite directions of the magnetic field guiding neutron spin. This field defines the neutron spin direction on the target. Switching the field direction should obviously change the sign of any real spin-dependent effects while systematic non-spin-dependent effects should stay the same. The guiding field was switched approximately once per day. Again, the final value of the asymmetry quoted was

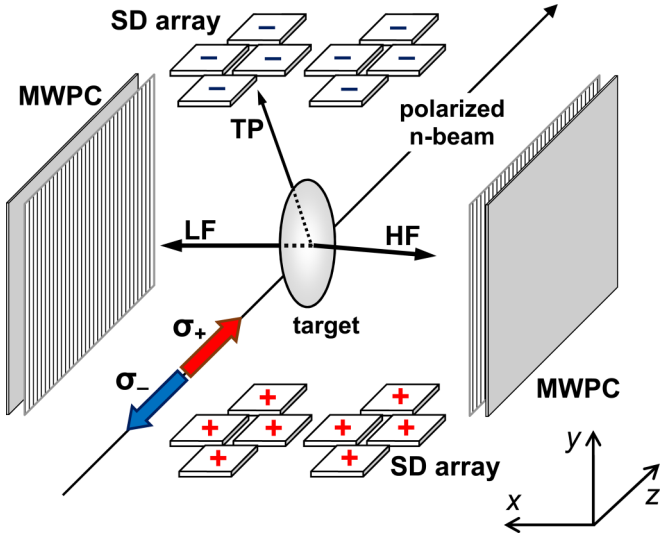

FIG. 2. Pattern of asymmetries in ^{233}U(n,f). As shown, the light fragment flies in the $+x$ direction and the ternary particles fly upwards with $y > 0$. The asymmetry A is $A < 0$.

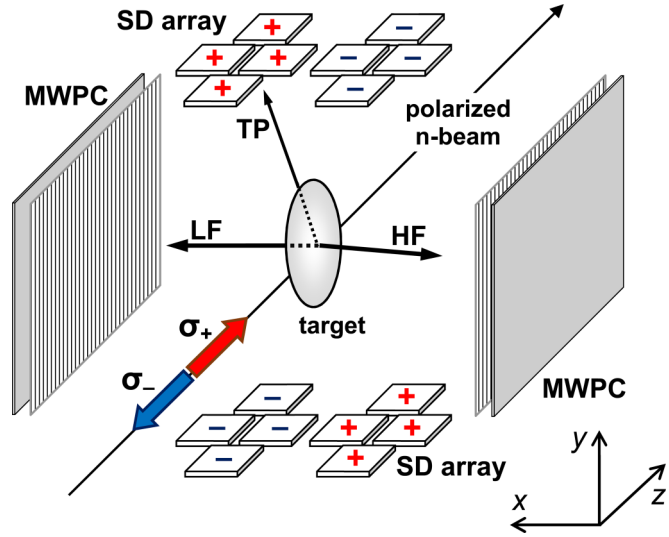

FIG. 3. Pattern of asymmetries in ^{235}U(n,f). The light fragment is flying to the left in the $+x$ direction.

obtained by averaging the opposite field measurements with proper switch in sign. By contrast, averaging data without change in sign yielded within statistical accuracy the asymmetry zero as expected in case of no false systematic effects.

In summary, from the analyses described we conclude that any false effects are definitely smaller than the statistical errors. The errors are shown in all following plots as error bars calculated from statistical accuracy. All error bars on experimental data points shown in the following plots were calculated from statistical accuracy.

III. EXPERIMENTAL RESULTS

From experiment the asymmetries A were evaluated according to Eq. (3). The first experiment was run with ^{233}U as the target in the polarized neutron beam. It became quickly evident that asymmetries were nonzero [8]. The signs of the asymmetries are on display in Fig. 2 for LFs flying in the $+x$ direction. The asymmetry A for the reference combination of ternary events is negative: $A < 0$. It is further observed that, when instead of the light fragments heavy ones are moving in the $+x$ direction the asymmetries A have signs opposite to Fig. 2. At a first look the pattern appears to be in agreement with the correlator B of Eq. (1) and the angular correlation of Eq. (2). However, the absolute size of the effect $|A| = 3.90(12) \times 10^{-3}$ is 10 times larger than the size of PNC effects measured in fission. It is hence by far larger than expected for violation of time reversal invariance. Further, a closer inspection reveals that the angular dependence $A \sim \sin(\theta_{\mathrm{TP-LF}})$ put forward by the correlator B is not observed. The name given to the phenomenon was "TRI effect" because it refers to a triple correlation between three variables $\boldsymbol{\sigma}_n$, $\mathbf{p}_{\mathrm{LF}}$, and $\mathbf{p}_{\mathrm{TP}}$. The challenge is to explain the effect without invoking the hypothetical correlation B of Eq. (1).

Polarized neutron induced fission of ^{235}U, the neighboring isotope to ^{233}U with two more neutrons, was investigated next. Surprisingly, as visualized in Fig. 3, the pattern of asymmetries for ^{235}U is very different from the one for ^{233}U [9,14]. This pattern definitely cannot be described by the correlator B of Eq. (1). Evidently there must be two different mechanisms at work leading to such widely different asymmetry patterns in neighboring isotopes. For reasons explained in the discussion below the name "ROT effect" was given to the present observation.

The intriguingly different observations in the two U isotopes motivated the systematic investigation of asymmetries in the major actinides. Results of these investigations are reported in the present work. A survey of asymmetries for the four target nuclei ^{233,235}U and ^{239,241}Pu is on display in Fig. 4. Detailed asymmetries as a function of the angle $\theta_{\mathrm{TP-LF}}$ between TP and LF are shown. Blue circles with error bars are experimental data. The histograms with scale to the right depict the angular distributions of ternary particles as measured in the present experiments. Because of the coarse granularity of TP detectors and the not perfect separation between LF and HF for the ^{239}Pu target the angular distribution is wider than in dedicated experiments. Note that in asymmetric fission the TPs are pushed by Coulomb forces towards the lighter fragment and on average the angle $\theta_{\mathrm{TP-LF}}$ is shifted from $\langle\theta_{\mathrm{TP-LF}}\rangle = 90^\circ$ in symmetric fission to $\langle\theta_{\mathrm{TP-LF}}\rangle \approx 82^\circ$. In the patterns of asymmetries the strongest contrast is between the target nuclei ^{233}U and ^{235}U. Note that in ^{233}U the asymmetry stays negative for all angles $\theta_{\mathrm{TP-LF}}$ while for all other reactions asymmetries are sloping downwards from positive to negative for angles $\theta_{\mathrm{TP-LF}}$ increasing.

The asymmetries discovered in TP emission disclose changes in the TP angular distributions depending on the orientation of the spin of neutrons inducing fission. Phenomenologically one may imagine two simple types of changes of TP emission patterns. They are illustrated in Fig. 5.

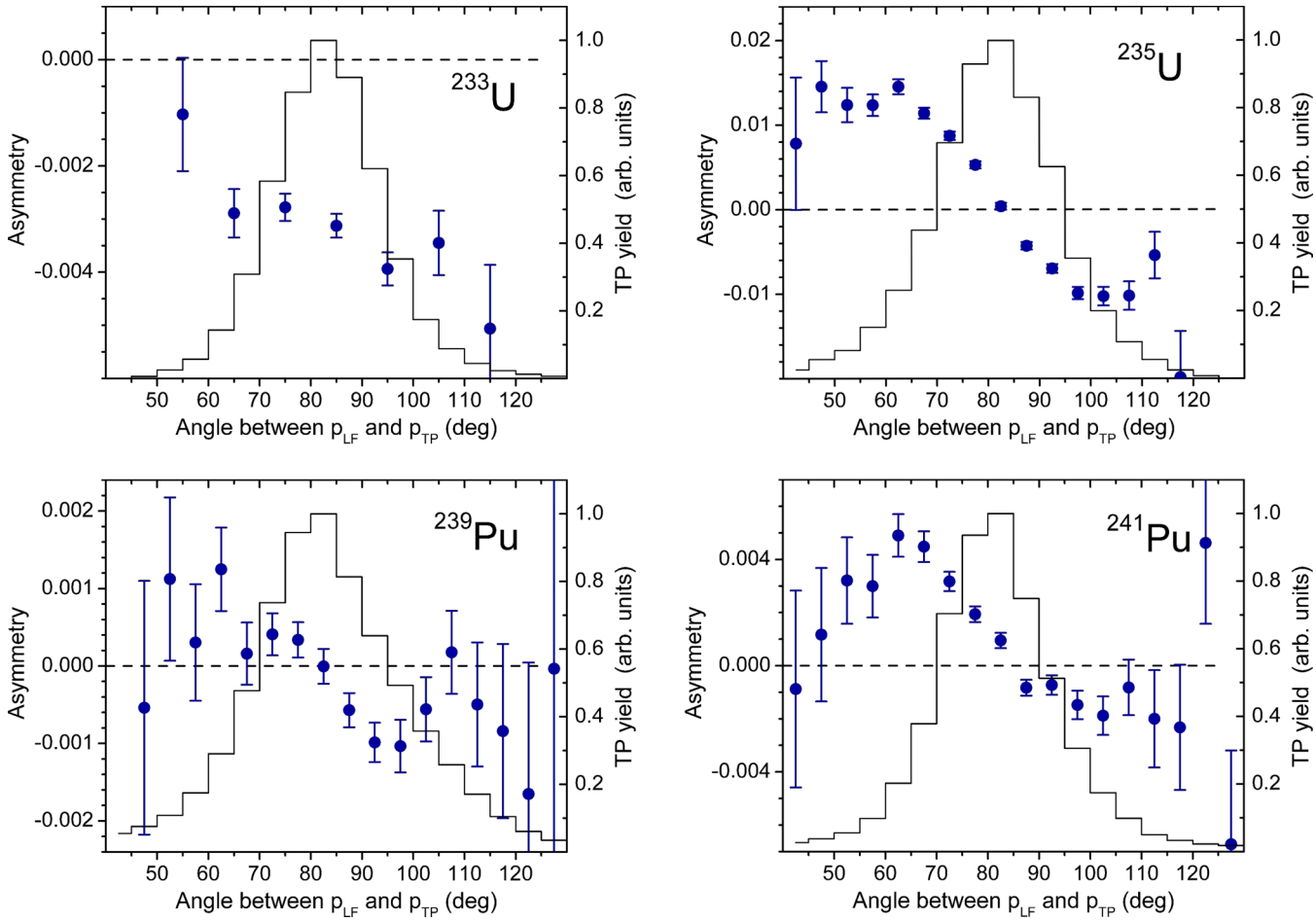

FIG. 4. Experimental asymmetry as a function of angle $\theta_{\mathrm{TP-LF}}$ for the four target nuclei $^{233,235}\mathrm{U}(n,f)$ and $^{239,241}\mathrm{Pu}(n,f)$ (blue circles with error bars). The dashed horizontal line indicates zero asymmetry $A = 0$. TP angular distributions are plotted as histograms with scale to the right. The asymmetries shown are for LF flying in Fig. 1 to the left ($+x$ direction) and TP upwards ($+y$ direction). Note the changes in scale for the different reactions and in particular the throughout negative sign of the asymmetry for $^{233}\mathrm{U}(n,f)$.

To be definite let us consider the reference combination of events in Fig. 1 with LF flying in the $+x$ direction and TP towards the upper hemisphere with $y > 0$. To the left of Fig. 5 it is assumed that the position and shape of the angular distribution between TP and LF remains unchanged when neutron spin is flipped. The two distributions differ only by

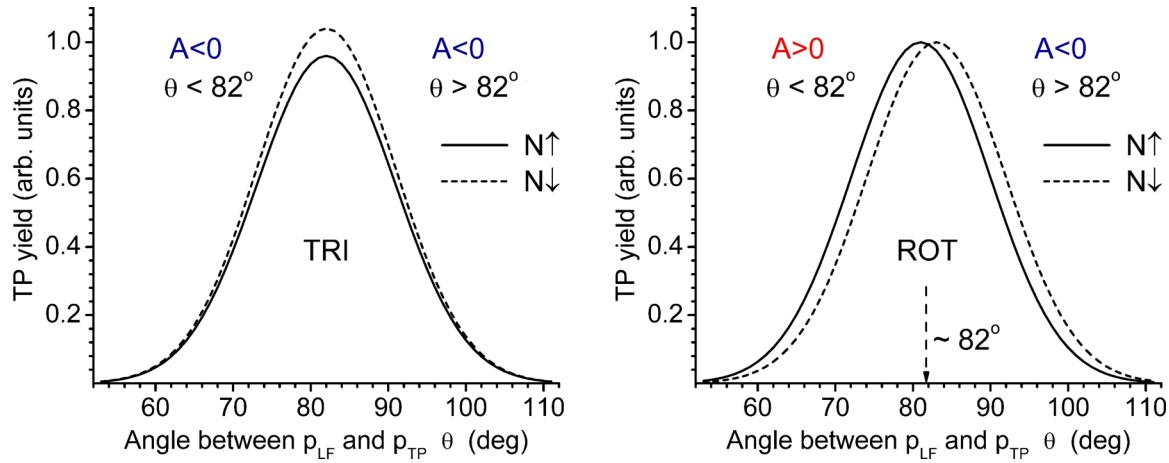

FIG. 5. Angular distributions of ternary particles in (n,f) reactions depending on orientation of neutron spin relative to $(\mathbf{p}_{\mathrm{LF}} \times \mathbf{p}_{\mathrm{TP}})$. $N_{\uparrow}$ and $N_{\downarrow}$ are emission rates for neutron spin parallel and antiparallel to $(\mathbf{p}_{\mathrm{LF}} \times \mathbf{p}_{\mathrm{TP}})$, respectively. TRI effect to the left, ROT effect to the right.

a constant factor of multiplication not depending on the angle $\theta_{\mathrm{TP-LF}}$. The asymmetries $A \sim (N_\uparrow - N_\downarrow)$ in Eq. (3) will then evidently have the same sign for all angles $\theta_{\mathrm{TP-LF}}$ as observed in Fig. 2 for the reaction $^{233}\mathrm{U}(n,f)$. This is characteristic for the TRI effect. In Fig. 5 the experimental signs for the TRI effect in the reference combination are reproduced for TP yields being larger for spin antiparallel ($N_\downarrow$) and smaller for spin parallel ($N_\uparrow$) to the beam running perpendicular to the ($\mathbf{p}_{\mathrm{LF}}$,$\mathbf{p}_{\mathrm{TP}}$) plane.

As sketched to the right in Fig. 5 the ROT effect is ventured to come about by angular shifts of the angular distribution of TPs as a whole. In the present experimental setup the angular distribution $N_\uparrow$ for spins parallel to the beam is shifted from the average value $\langle\theta_{\mathrm{TP-LF}}\rangle \approx 82^\circ$ to smaller angles and for inverted spin the distribution $N_\downarrow$ is pushed to larger angles. The sign of the asymmetry $A \sim (N_\uparrow - N_\downarrow)$ then is positive for angles $\theta_{\mathrm{TP-LF}}$ smaller and negative for angles larger than the average 82°. This is in fact the pattern of asymmetries for the ROT effect observed in experiment in Fig. 3 for the reaction $^{235}\mathrm{U}(n,f)$.

The challenge then is developing models which may explain why and how two different types of effects affecting the angular distributions for ternary particles are coming about, both being steered by the spin orientation of neutrons inducing fission. One may venture that in general the two effects are superimposed. Because it turns out that in particular the ROT effect can be understood in a simple semiclassical model, first the ROT effect is discussed in the next chapter.

IV. MODEL FOR THE ROT EFFECT

The asymmetries discovered are discussed in the frame of the theory for fragment angular distributions. The theory was devised by A. Bohr introducing transition states at the fission barrier as channels for fission [15]. The theory has found many applications [16]. It has to be recalled and underlined that for low energy neutron fission of fissile nuclei like $^{233,235}\mathrm{U}$ and $^{239,241}\mathrm{Pu}$ presently studied all the available states near the saddle point of fission are collective in nature. There is just not enough energy available to break nucleon pairs and excite single particle states. At the saddle point the deformed nucleus is described by the wave function of a spinning top D_{JMK}. The good quantum numbers are J, M, and K with **J** the angular momentum, **M** its projection on a space fixed axis z, and **K** the projection of **J** on the fission axis. The classical breakdown of **J** into **K** and the component **R** perpendicular to the fission axis is visualized in Fig. 6. It is generally assumed that not only **J** but also the component **K** is conserved from saddle to scission.

Shortly after discovering the TRI effect it was suggested that rotations of fissioning nuclei may be the source of the new phenomena [17]. The later observation of the ROT effect corroborated this conjecture [9,14]. Collective rotations of fission prone nuclei come in experiment into view for polarized nuclei. The phenomenological model to be discussed in the following starts from the assumption that the collective rotation R perpendicular to the fission axis is crucial for the ROT effect. In the model ternary particles are expelled at scission from the neck of a strongly deformed and rotating nucleus.

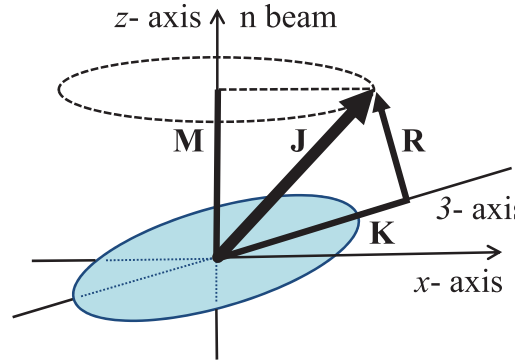

FIG. 6. Classical decomposition of total angular momentum **J** into the components **K** along the axis of deformation (fission axis) and **R** perpendicular to this axis. The projection of **J** on a space fixed z axis is M.

To simplify arguments near-symmetric fission is considered with the TP being emitted at right angles to the fission axis as sketched in Fig. 7. After scission the rotation in the physical sense of the word ceases but the composite system continues to turn around. The turning of the fission axis joining the two fragments in binary fission is a consequence of the start velocities of fragments being ejected at scission from a rotating system. In the absence of Coulomb forces the fragments would continue to move on parallel but staggered straight trajectories and for fragments at infinity the fission axis would have turned around by 90°. However, after scission the strong Coulomb

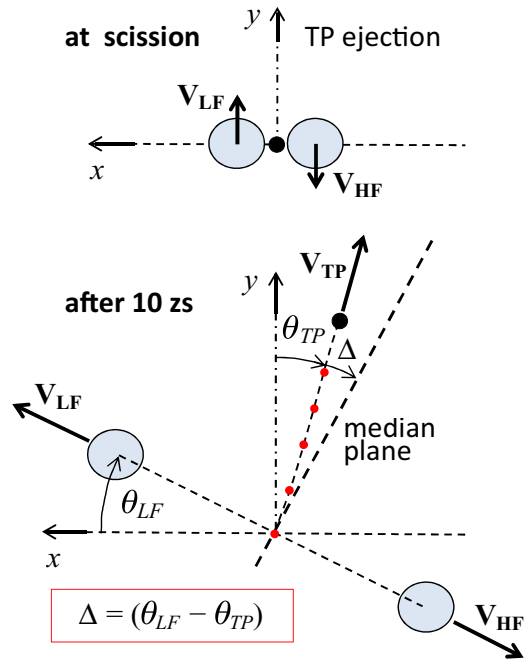

FIG. 7. Model of ROT effect. In near-symmetric fission the TP is ejected at right angles to the fission axis from a rotating compound (rotation assumed clockwise). After scission the fission axis continues to turn entraining the TP trajectory. After a few zs the Coulomb forces no longer keep the TP on a median plane perpendicular to the instantaneous fission axis. A lag angle $\Delta = (\theta_{\mathrm{LF}} - \theta_{\mathrm{TP}}) > 0$ develops.

force between the two fragments vehemently accelerates them virtually along the fission axis. The angular speed of rotation of the fission axis is hence getting smaller and smaller and the revolution of the fragments comes virtually to a stop in few zs. Corroborated by trajectory calculations the turning angle of the fission axis is less than one degree. Note that upon flipping the nuclear polarization the sense of rotation is reversed.

In ternary fission the situation is more entangled. The fission axis becomes slightly bent from the impact of the ternary particle. This bending is neglected in Fig. 7. To understand how the ROT effect is coming about it has to be kept in mind that Coulomb forces exerted by the two fragments on ternary particles are trying to keep the TP on a median plane perpendicular to the instantaneous fission axis. With the fission axis rotating also the median plane is turning around by the same angle. However, with all three particles flying apart the Coulomb forces fade away and after a few zs no longer fully can bend the trajectory of the TP. Because of inertia the TP will stay behind the turning median plane. As illustrated in Fig. 7 the turning angle $\theta_{\rm LF}$ of the fission axis is therefore larger than the turning angle of the TP trajectory $\theta_{\rm TP}$. A lag angle $\Delta > 0$ develops between the two angles:

$$\Delta = \theta_{\rm LF} - \theta_{\rm TP}. \tag{4}$$

For the reference emission pattern with LF in $+x$ and TP in $+y$ direction (see Fig. 1) the angle of observation $\theta_{\rm LF-TP}$ between the momenta of TP and LF in Fig. 7 is shifted to smaller emission angles. Inverting the sense of rotation the angle $\theta_{\rm LF-TP}$ is shifted to larger angles. In experiment the sense of rotation of the compound nucleus is controlled by the orientation of the spins of neutrons inducing fission, $\boldsymbol{\sigma}_\uparrow$ or $\boldsymbol{\sigma}_\downarrow$. It is given by the sign of the angular velocity ω_z around the z axis in Fig. 1. For capture states with $J_+ = (I + 1/2)$ the sense of rotation is positive or negative for neutron spin along or against beam direction $\boldsymbol{\sigma}_\uparrow$ or $\boldsymbol{\sigma}_\downarrow$, respectively. For capture states $J_- = (I - 1/2)$ the signs are inversed. Thereby J is the compound spin and I the target spin. Because in evaluating the asymmetry A from Eq. (3) the difference between the two spin orientations is taken, the shift observed between the two angular distributions of TPs when spin is flipped amounts to 2Δ. It is precisely this shift 2Δ between angular TP distributions which is shown to the right in Fig. 5 for asymmetric fission assuming neutron capture with $J_+ = (I + 1/2)$. Near the peak of the TP angular distribution at $\theta_{\rm LF-TP} \approx 82^\circ$ the asymmetry $A \sim (N_\uparrow - N_\downarrow)$ becomes nil because $N_\uparrow \approx N_\downarrow$. For angles $<82^\circ$ or $>82^\circ$ the sign of the asymmetry changes. These features explain surprisingly well the results for the asymmetry in Fig. 3. The angular shifts $\pm\Delta$ of TP distributions appear hence to be the basic phenomenon steering the ROT effect. This success of the rotational model for the interpretation of the ^{235}U experiment justifies the name "ROT" effect given to the phenomenon. It is finally worth pointing out that the ROT shift of TP angular distributions is only observable because the angular distribution of TPs is not isotropic but squeezed into a narrow cone near the angle $\langle\theta_{\rm LF-TP}\rangle \approx 82^\circ$.

The phenomenological model just outlined accounts well for the general features of the ROT effect but as to size quantitative Monte Carlo trajectory calculations had to be performed. In these calculations first the starting conditions had to be determined reproducing the best well-known energy and angular distributions of ternary particles for a nonrotating system. They were then generalized to take into account the rotation of the fissioning system at scission. Details on the starting parameters at scission are to be found in Refs. [18,19].

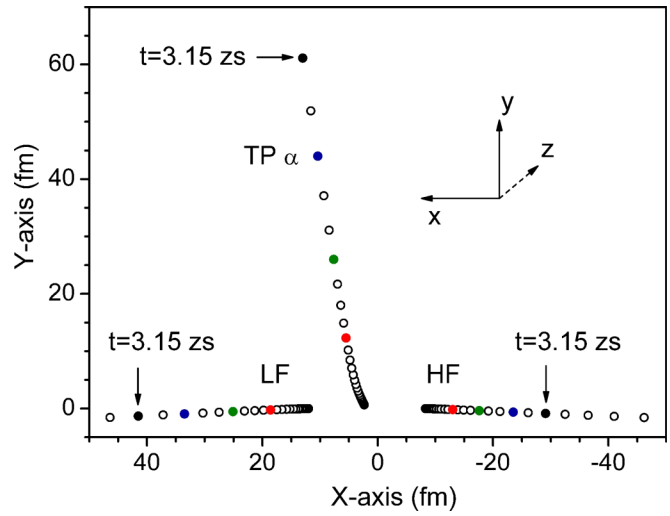

FIG. 8. Trajectories of fragments and ternary α particle from ternary fission of ^{236}U*.

Figure 8 shows an example of a trajectory calculation for a nonrotating nucleus in ternary fission. Remarkably the three particles involved have moved away from the center of fission by 30–60 fm in times of only 3 zs. It should also be noted that as to be expected the bending of the TP trajectory (in the figure an α particle) is only effective on the first few fm of the trajectory. It is further seen that for asymmetric fission the TP is pushed away from the heavier fragment HF towards the light fragment LF. The average angle $\theta_{\rm TP-LF}$ of TP emission is hence smaller than 90° and comes close to 82°.

For a detailed calculation of trajectories in case of TP emission from a rotating composite system the size of the angular velocity component $\omega_z(J,K)$ at scission has to be known for given angular momentum $\mathbf{J}$ and its component K. A quantum-mechanical derivation was given in Ref. [20]. The angular velocity is linked to the average component $\langle J_z(J,K)\rangle$ of the angular momentum along the z direction of the beam by

$$\omega_z(J,K) = \frac{\langle J_z(J,K)\rangle}{\Im_z} \tag{5}$$

with $\Im_z$ the moment of inertia around the z axis in the scission configuration. Theory yields

$$\omega_{z+}(J,K) = +\frac{p_n\hbar}{2\Im_z} \times \frac{J(J+1) - K^2}{J},$$
$$\omega_{z-}(J,K) = -\frac{p_n\hbar}{2\Im_z} \times \frac{J(J+1) - K^2}{J+1}, \tag{6}$$

with $p_n = \langle\sigma_z\rangle/\sigma$ the neutron polarization along the z axis of the neutron being absorbed, and ω_{z+} and ω_{z-} correspond to the $J_+ = (I + 1/2)$ and $J_- = (I - 1/2)$ capture states, respectively. It should be noted that depending on the orientation

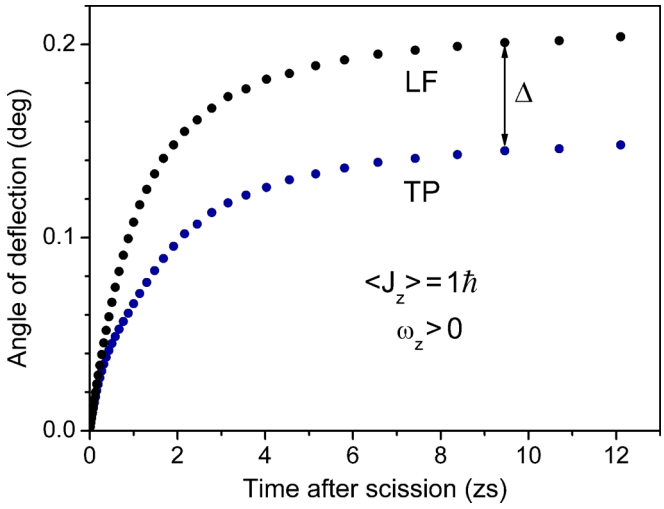

FIG. 9. Deflection angle $\theta_{\rm LF}$ of light fragment LF and deflection angle $\theta_{\rm TP}$ of ternary particle TP as a function of time in units of zs for $\langle J_z\rangle = 1\,\hbar$. The lag angle Δ is the difference of angles $(\theta_{\rm LF} - \theta_{\rm TP})$.

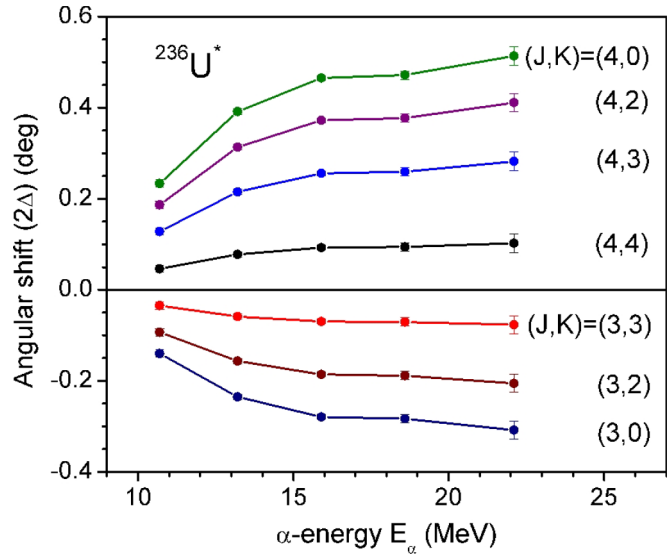

FIG. 10. Angular ROT shift 2Δ in the reaction $^{235}{\rm U}(n,f)$ as a function of ternary α-particle energy E_α for given quantum numbers (J,K) of transition states.

of neutron spin $\sigma_z = \pm\frac{1}{2}\hbar$ pointing in or against the direction of the neutron beam (in Fig. 1 the z axis), the polarization p_n is positive or negative, respectively.

To give a typical example, the deflection angles $\theta_{\rm LF}$ and $\theta_{\rm TP}$ of the light fragment and the ternary particle, respectively, are on display in Fig. 9 as a function of time. For the calculation the angular momentum around the z axis was assumed to be $\langle J_z\rangle = 1\,\hbar$. Once more it is observed in Fig. 9 that already in a few zs the TP trajectory lags behind the LF in turning angle. The final lag angle Δ is reached in only $\approx$4 zs. The angular TP distribution is hence shifted compared to a nonrotating composite system. It is also surprising that in about 10 zs the trajectories are virtually no longer turning but become stationary in space. But the most important information from the figure are the sizes of the turning angles $\theta_{\rm LF}$ and $\theta_{\rm TP}$, and the lag angle $\Delta = (\theta_{\rm LF} - \theta_{\rm TP})$. The order of magnitude of the lag angle is $\Delta \approx 0.1^\circ$ for $\langle J_z\rangle = 1\,\hbar$. The calculations further bring to evidence that to good accuracy the shift angle Δ is proportional to the angular velocity $\omega_z(J,K)$. Because in experiment according to Fig. 5 the difference 2Δ in lag angles is found by observing the asymmetry A for the two spin flipped situations, the relation between 2Δ and $\omega_z(J,K)$ is written as

$$2\Delta = c_1\omega_z(J,K), \tag{7}$$

with the factor c_1 found by trajectory calculations in the frame of the model.

For direct comparison with experiment the angular shift differences 2Δ of TP angular distributions are calculated as a function of the TP energy with TP taken to be an α particle. The angular velocities $\omega_z(J,K)$ of the compound nucleus at the moment of scission are obtained from Eq. (6). Thereby the moment of inertia $\Im_z$ was calculated for the scission configuration best fitting energy and angular distributions of ternary α particles. The result for $^{236}{\rm U}^*$ is plotted in Fig. 10.

In the figure the ROT shift 2Δ varies strongly with the (J,K) value adopted. It changes sign for $J = J_+$ or $J = J_-$. This result is as anticipated in the phenomenological model. The shift is largest in magnitude for states $(J,0)$ with $K = 0$. Because $R(R+1) = J(J+1) - K^2$ states with $K = 0$ correspond to maximum rotational angular momentum **R** around the axis of polarization. Again this is in line with expectation from the phenomenological model. Except for isolated resonances in the fission cross section, both compound spin states J_+ and J_- will in experiment be present at any neutron energy. The two contributions cannot be disentangled in experiment and therefore an effective shift 2Δ is observed weighted by the spin-dependent cross sections $\sigma_f(J_+)$ and $\sigma_f(J_-)$, respectively. To make the analysis tractable it is assumed that for each spin only one state (J,K) has to be taken into account. This simplification is justified but may not always be fulfilled. The effective shift 2Δ then is

$$2\Delta = c_1\left[\omega_{z+}(J_+,K_+)\frac{\sigma_f(J_+)}{\sigma_f(J_+)+\sigma_f(J_-)} + \omega_{z-}(J_-,K_-)\frac{\sigma_f(J_-)}{\sigma_f(J_+)+\sigma_f(J_-)}\right]. \tag{8}$$

In experiment it is the asymmetry A which is measured, defined as $A = (N_\uparrow - N_\downarrow)/(N_\uparrow + N_\downarrow)$ in Eq. (3). Recalling Fig. 5, the asymmetry A for the ROT effect $A_{\rm ROT}(\theta_{\rm TP-LF})$ depending on angle $\theta_{\rm TP-LF}$ is readily found to be

$$A_{\rm ROT}(\theta_{\rm TP-LF}) = 2\Delta\frac{Y'(\theta_{\rm TP-LF})}{2Y(\theta_{\rm TP-LF})}. \tag{9}$$

In Eq. (9) $Y(\theta_{\rm TP-LF})$ is the angular distribution of ternary particles as a function of the angle $\theta_{\rm TP-LF}$ as measured in experiment. The slope of the distribution Y becomes $Y'(\theta_{\rm TP-LF}) = 0$ at the peak of the distribution for $\theta_{\rm TP-LF} \approx 82^\circ$. At this angle $A_{\rm ROT} = 0$ and hence there is no contribution to the asymmetry A from the ROT effect. Note that the formula describes the asymmetry for the reference configuration with LF flying in Fig. 3 in the $+x$ direction to the left and TP upwards in the direction of the $+y$ axis.

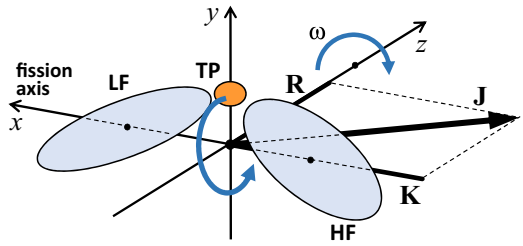

FIG. 11. Model for K states of a nucleus with broken axial symmetry about to undergo ternary fission. The TP is kept between the tips of the nascent fragments. Because of an additional rotation with angular velocity $\boldsymbol{\omega}$ perpendicular to the fission axis a Coriolis force is exerted on the TP.

V. MODEL FOR THE TRI EFFECT

Having demonstrated that the ROT effect is satisfactorily understood by attributing it to the **R** component of angular momentum **J**, it is tempting to conjecture that the TRI effect may sense the projection K of **J** on the fission axis. As repeatedly pointed out all near-barrier (J,K) states of even-even nuclei studied in the present experiments are collective. In particular this entails that any $K > 0$ states of rotation around the fission axis are only feasible provided the nucleus is no longer axially symmetric. A nuclear model with broken axial symmetry being well adapted to the process of fission is proposed.

Nonaxial oscillations of a nucleus near the scission point were first discussed in 1965 [21]. In particular so-called bending modes were studied in the theory of angular momentum of fragments [22,23]. Bending modes were introduced as vibrational modes in two planes perpendicular to each other, one in the (x,y) plane and another one in the (x,z) plane of Fig. 11. The two planar vibrations are degenerate in energy. They may equally well be described as rotations of a permanently bent nucleus around the x axis connecting the centers of mass of the two fragments. There are two rotations with opposite senses of rotation. They carry projections of angular momenta $+K$ and $-K$ along the fission axis. Their probability to be excited is equal, and again the two states are degenerate. Loosely speaking the motion is reminiscent of "rotating bananas." The model describes classically the angular momentum around the axis connecting the two fragments. On time average the axial symmetry is restored.

Turning to ternary fission, the TP is assumed to sit in the neck between the tips of the fission prone fragments. The TP participates in the banana rotation and is moving up and down with velocity $v_{\rm TP}$ up- and downwards along the y axis in Fig. 11. According to Eq. (6) there is in addition even in the limiting case of $K = J$ a nonzero rotation of the composite nucleus with angular velocity $\boldsymbol{\omega}$ around the z axis. Therefore the TP experiences a Coriolis force $\mathbf{F} \sim (\mathbf{v}_{\rm TP} \times \boldsymbol{\omega})$ acting along the x axis in Fig. 11. The angular velocity $\boldsymbol{\omega}$ has only one component ω_z around the z axis. It is inverted when the spin of the neutron inducing fission is flipped. As a result also the force **F** will be inverted. Depending on whether the TP is moving up or down with $\mathbf{v}_{\rm TP}$ the Coriolis force may either hinder or favor cutting the bond between the TP and the fragment to which the TP is still clinging. Thus an asymmetry in the emission yield of ternary particles emerges but with opposite signs in the upper or lower hemisphere of Fig. 11. This is in Fig. 2 the essence of the TRI effect.

The present model is based on the Coriolis force steering the emission probability of TPs. There is no obvious reason to introduce a dependence of the TRI effect on the angle $\theta_{\rm TP-LF}$ between TP and LF because the angular distribution is fashioned at a later stage by Coulomb forces. On the other hand, one would expect a sine dependence on the angle between $(\mathbf{p}_{\rm TP} \times \mathbf{p}_{\rm LF})$ and $\boldsymbol{\omega}$. In the experimental setup the angle between the plane $(\mathbf{p}_{\rm TP} \times \mathbf{p}_{\rm LF})$ and the angular velocity $\boldsymbol{\omega}$ lies in a narrow range centered at 90°. For events where the plane $(\mathbf{p}_{\rm TP} \times \mathbf{p}_{\rm LF})$ is not perpendicular to $\boldsymbol{\omega}$ a geometrical correction was applied in the evaluation of data. We may therefore only consider the angular dependence between the momenta $\mathbf{p}_{\rm TP}$ and $\mathbf{p}_{\rm LF}$ in the plane perpendicular to $\boldsymbol{\omega}$ and write for the angular distribution $W(\mathbf{p}_{\rm TP},\mathbf{p}_{\rm LF})$ in polarized neutron fission,

$$W(\mathbf{p}_{\rm LF},\mathbf{p}_{\rm TP}) \sim (1 \pm D)W_0(\mathbf{p}_{\rm LF},\mathbf{p}_{\rm TP}), \tag{10}$$

with D a constant representing the size of the TRI asymmetry; plus and minus in the formula correspond to $\boldsymbol{\sigma}_n \cdot (\mathbf{p}_{\rm LF} \times \mathbf{p}_{\rm TP}) > 0$ and $\boldsymbol{\sigma}_n \cdot (\mathbf{p}_{\rm LF} \times \mathbf{p}_{\rm TP}) < 0$, respectively. In the spirit of the model the TRI asymmetry is conjectured to be proportional to the Coriolis force $F \sim |(\mathbf{v}_{\rm TP} \times \boldsymbol{\omega})| = v_{\rm TP}\omega_z$ because $\mathbf{v}_{\rm TP} \perp \boldsymbol{\omega}$ and therefore

$$D \sim v_{\rm TP}\omega_z. \tag{11}$$

For the evaluation the velocity $\mathbf{v}_{\rm TP}$ of the TP is parametrized by the K quantum number. Consistent with the model the assumption behind is that the velocity $\mathbf{v}_{\rm TP}$ and the K quantum number are proportional to each other. The angular velocity $\boldsymbol{\omega}$ in the formula for the Coriolis force has the only component $\omega_z(J,K)$ from Eq. (5) around the beam z axis. Taking into account the contributions of the two capture states J_+ and J_- weighted by their spin-dependent fission cross sections $\sigma_f(J_+)$ and $\sigma_f(J_-)$, the TRI effect parameter D becomes with a constant c_2,

$$D = c_2\Bigg[K_+\omega_{z+}(J_+,K_+)\frac{\sigma_f(J_+)}{\sigma_f(J_+)+\sigma_f(J_-)} + K_-\omega_{z-}(J_-,K_-)\frac{\sigma_f(J_-)}{\sigma_f(J_+)+\sigma_f(J_-)}\Bigg]. \tag{12}$$

The K numbers have to be taken as those evaluated for the ROT effect. The angular velocities ω_z depending on K were taken from Eq. (6). The signs for ω_{z+} and ω_{z-} are inverted and accordingly also the two terms in Eq. (12) have opposite signs.

It has further to be stressed that in a double neck rupture model the sign of the TRI asymmetry D will be different for the TP being ejected either from the heavy or the light fragment. In double neck rupture models of ternary fission it is usually assumed that first the heavy fragment with a stiff ^{132}Sn core is set free [24]. For the second neck rupture the complementary deformed light fragment has a bulge as the precursor of a ternary particle. Without rotation all three particles are aligned along the fission axis. In the following discussion it is taken for granted that in the majority of cases the ternary particle

has to be set free by the light fragment. It is here that the advocated Coriolis force comes into play. With the sequence of neck ruptures advocated the sign of the constant prefactor c_2 in Eq. (12) is negative, because for the reference emission pattern with the LF flying in the $+x$ direction, the TP in the $+y$ direction and with $\omega_z > 0$ the Coriolis force will act in the $+x$ direction and hence hinder the TP to be detached from its mother nucleus. Remarkably, for all four reactions studied the sign of the TRI asymmetry is correctly predicted. As to size the prefactor c_2 was calibrated by resorting to the best studied reaction $^{235}\mathrm{U}(n,f)$ from a fit to the measured TRI asymmetry. This constant was adopted for all other reactions studied.

From Eqs. (3) and (10) it follows that the experimental asymmetry A_{TRI} and the TRI parameter D are simply equal:

$$A_{\mathrm{TRI}} = D. \tag{13}$$

VI. EVALUATED RESULTS

The analysis of experimental results was guided by the models for the ROT and the TRI effect. It has first to be recalled that both effects contribute in all reactions investigated. The asymmetry $A(\theta_{\mathrm{TP-LF}})$ observed is, hence,

$$A(\theta_{\mathrm{TP-LF}}) = A_{\mathrm{ROT}}(\theta_{\mathrm{TP-LF}}) + A_{\mathrm{TRI}}, \tag{14}$$

where $A_{\mathrm{ROT}}(\theta_{\mathrm{TP-LF}})$ is given by Eq. (9) and A_{TRI} by Eq. (13).

Several corrections had to be applied to the experimental raw data. In addition to the evident correction for finite neutron polarization, which was determined for each run with an accuracy not worse than 2%, accidental coincidences between fragments and ternary particles were measured in staggered time windows excluding real events. Especially for the Pu data where only one fragment could be intercepted, a correction for HFs being wrongly assessed as LFs was necessary. The correction depends on the angle $\theta_{\mathrm{LF-TP}}$ and it was calculated in a Monte Carlo simulation of the experiment. A further correction was required for events where the plane $(\mathbf{p}_{\mathrm{LF}}, \mathbf{p}_{\mathrm{TP}})$ was not perpendicular to neutron spin. The geometric correction factor was again found by a Monte Carlo simulation. The angular distributions $Y(\theta_{\mathrm{TP-LF}})$ of TPs were determined as the average of angle-dependent count rates for the two neutron spin orientations corrected for the efficiency of ternary fission detection in the particular layout of each experiment.

Based on the models the separate identification of ROT and TRI effects in the experimental plots of asymmetries $A(\theta)$ of Fig. 4 is straightforward. Experimental asymmetries with all corrections included were fitted by the model function of Eq. (14) with the two terms given in Eqs. (9) and (13). For all reactions studied the parameters 2Δ and D were obtained from fits based on a χ^2 minimization with only these two parameters being free.

Experimental results for the asymmetry $A(\theta_{\mathrm{TP-LF}})$ were already shown in Fig. 4 for the four fission reactions studied. Comparisons of experiments and models are presented in Fig. 12. Blue circles with error bars are from experiment. Results of the evaluation outlined are inserted as red squares. Evidently the models give an excellent description of the experimental findings. As already noticed in the discovery experiments, in the reaction $^{235}\mathrm{U}(n,f)$ the ROT effect and in the reaction $^{233}\mathrm{U}(n,f)$ the TRI effect are dominant. This is inferred from the angular dependence of the asymmetry $A(\theta_{\mathrm{TP-LF}})$ which for $^{235}\mathrm{U}(n,f)$ is very pronounced and changing sign as a function of $\theta_{\mathrm{LF-TP}}$ as anticipated for the ROT effect. By contrast, in the companion reaction for the isotope $^{233}\mathrm{U}$, the throughout negative sign of the asymmetry in Fig. 4 signals a prevailing TRI effect with only a minor contribution from the ROT effect. Notably a fair agreement between experiment and theory is achieved by taking into account for the ROT effect the dependence of the asymmetry on the slope of the angular distributions $Y(\theta_{\mathrm{TP-LF}})$ of TPs as proposed in Eq. (9). In all four reactions scrutinized the asymmetry slopes downwards from maxima to minima across the angular TP distributions shown as histograms with scale to the right. The extremes are observed at angles $\theta_{\mathrm{TP-LF}}$ where the slopes of the angular distribution are largest positive or negative, respectively. At very small or large angles $\theta_{\mathrm{TP-LF}}$ of the distribution $\mathrm{Y}(\theta_{\mathrm{TP-LF}})$ the slopes become gentler and the asymmetries become smaller in magnitude. The dependence on slope gives the asymmetry curve $A_{\mathrm{ROT}}(\theta_{\mathrm{TP-LF}})$ a characteristic shape. The value D of the pure TRI effect can be read in Fig. 12 at the peak angle $\theta_{\mathrm{TP-LF}} \approx 82^\circ$ of the yield distribution where the derivative $Y'(\theta_{\mathrm{TP-LF}})$ vanishes.

The dependence of ROT and TRI effect parameters on the (J,K) quantum numbers prevailing at the saddle point of fission is exploited in the analysis to determine their values. The pertinent equations are given in Eq. (8) for the ROT and in Eq. (12) for the TRI effect. As already shown in Fig. 10, the angular shift 2Δ for the ROT effect depends sensitively on (J,K) quantum numbers and spin-dependent fission cross sections σ_f. To calculate the shift 2Δ requires in Eq. (7) the constant c_1 to be known. Trajectory calculations to find this constant were performed for a range of scission configurations for varying fragment mass ratios, tip distances, and start velocities. Those configurations were selected reproducing best energy and angular distributions of TPs. With Eq. (8) the ROT shift is a function of the compound spins J_+ and J_-, the K quantum numbers K_+ and K_-, and the fission cross sections $\sigma_f(J_+)$ and $\sigma_f(J_-)$. Even for $^{235}\mathrm{U}(n_{th},f)$ the spin-separated cold neutron fission cross sections are not well known from experiment [1,2]. For the evaluation cross sections communicated by A. B. Popov were used [25]. The angular shift was calculated for all (J,K) combinations and the results compared to the experimental value $2\Delta = 0.215(5)^\circ$. All pointed to the (J,K) combination $(J_+,K_+) = (4,0)$ together with $(J_-,K_-) = (3,2)$ as the optimum choice bringing the shift difference 2Δ close to experiment.

The shifts 2Δ calculated for all (J,K) combinations in $^{235}\mathrm{U}(n,f)$ are on display for comparison with the experimental shift $2\Delta = 0.215(5)^\circ$ in Table I. For Table I the scission configuration close to the anticipated average configuration was selected where the above (J,K) combination is in perfect agreement with experiment. We recall that for each spin value only one state (J,K) was taken into account. A similar analysis was performed for the TRI data from $^{235}\mathrm{U}(n,f)$. Thereby it has first to be recalled that the constant prefactor c_2 in Eq. (12) was adjusted as to size to reproduce the $^{235}\mathrm{U}(n,f)$ asymmetries with the superposition of (J,K) channels (4,0) and (3,2). Second, according to the TRI model introduced,

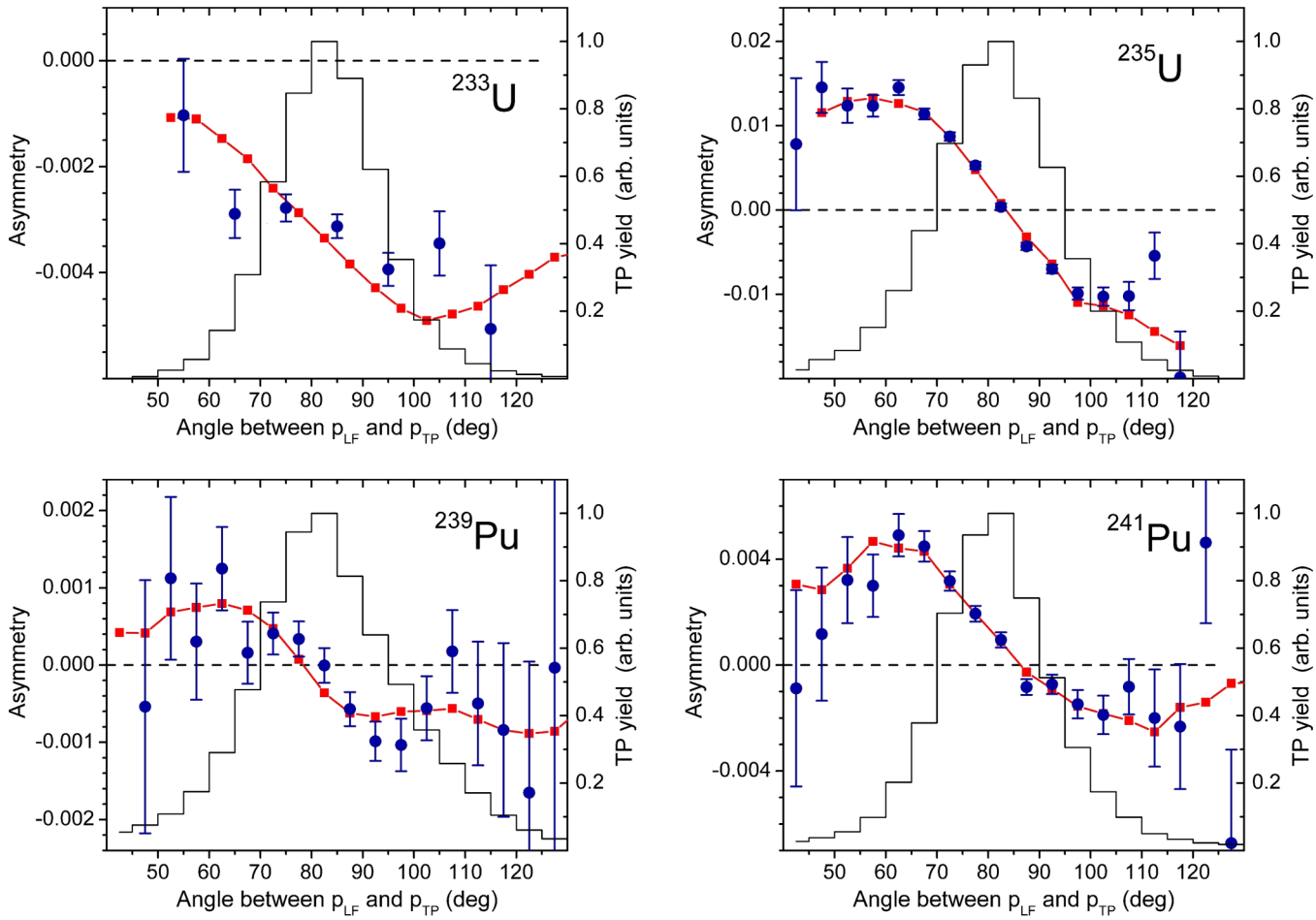

FIG. 12. Experimental asymmetries $A(\theta_{\mathrm{TP-LF}})$ for the four reactions studied (blue circles with error bars). Evaluated asymmetries (red squares). Angular distributions $W(\theta_{\mathrm{TP-LF}})$ of ternary particles (histograms with scale to the right). The asymmetries shown are for LF flying in Fig. 1 to the left ($+x$ direction) and TP upwards ($+y$ direction).

the $(J_+,K_+)=(4,0)$ state advocated in the ROT analysis is sterile for TRI because $K=0$. Only the state $(J_-,K_-)=(3,2)$ yields a contribution. With Eq. (12) experiment then tells that the sign of c_2 is negative. This same prefactor c_2 was adopted for all (J,K) combinations. Results of the (J,K) analysis are collected in Table II for comparison with the experimental value $D=+1.7(2)\times 10^{-3}$.

Asymmetries in the Table II are quoted as $D\times 10^3$. The perfect agreement between experiment and model for the combination of transition states $(J_+,K_+)=(4,0)$ together with $(J_-,K_-)=(3,2)$ is artificial because it was used to fix the constant prefactor in Eq. (12). The interesting information to be read from Table II is that for all other (J,K) combinations the calculated asymmetries are far away from experiment and in particular all nonzero K values for $J_+=4^-$ can be excluded. Therefore the assignments $(J_+,K_+)=(4,0)$ and $(J_-,K_-)=(3,2)$ inferred from the ROT effect is confirmed by the TRI effect.

The parameters 2Δ and D of the ROT and TRI effect, respectively, for the other reactions investigated were analyzed

TABLE I. ROT (J,K) analysis of 2Δ for $^{235}\mathrm{U}(n,f)$.

Target spin parity $I=7/2^-$; $\frac{\sigma_f(J_+=4)}{\sigma_f(J_-=3)}=1.76$

(J_+,K_+) \ (J_-,K_-)	(3,0)	(3,1)	(3,2)	(3,3)
(4,0)	0.183	0.191	**0.215**	0.255
(4,1)	0.169	0.177	0.201	0.241
(4,2)	0.128	0.135	0.159	0.199
(4,3)	0.058	0.066	0.090	0.129
(4,4)	−0.040	−0.032	−0.008	0.032

TABLE II. TRI (J,K) analysis of D for $^{235}\mathrm{U}(n,f)$.

Target spin parity $I=7/2^-$; $\frac{\sigma_f(J_+=4)}{\sigma_f(J_-=3)}=1.76$

(J_+,K_+) \ (J_-,K_-)	(3,0)	(3,1)	(3,2)	(3,3)
(4,0)	0.0	1.2	**1.7**	1.0
(4,1)	−3.5	−2.4	−1.8	−2.6
(4,2)	−6.0	−4.8	−4.3	−5.0
(4,3)	−6.1	−5.0	−4.4	−5.2
(4,4)	−3.0	−1.8	−1.3	−2.0

TABLE III. ROT (J,K) analysis of 2Δ for ^{233}U(n,f).

Target spin parity $I = 5/2^+-$; $\frac{\sigma_f(J_+=3)}{\sigma_f(J_-=2)} = 1.27$			
(J_+,K_+) \ (J_-,K_-)	(2,0)	(2,1)	(2,2)
(3,0)	0.118	0.131	0.170
(3,1)	0.102	0.115	0.153
(3,2)	0.053	0.066	0.105
(3,3)	−0.028	−0.015	0.023

following the scheme outlined for the ^{235}U(n,f) reaction adopting the calibrating constants c_1 and c_2 from this latter reaction. Difficulties encountered were from uncertainties in our knowledge of spin-dependent fission cross sections. For ^{233}U(n,f) and ^{239}Pu(n,f) ratios of cross sections were communicated in Ref. [26] based on evaluated nuclear data files in ENDF/B-VI.

Tables like the ones shown for the transition states from the ROT and TRI effect in ^{235}U(n,f) are given in Tables III–VIII for ^{233}U(n,f), ^{239}Pu(n,f), and ^{241}Pu(n,f). For the reaction ^{241}Pu(n,f) the cross-section ratio had to be determined as an additional parameter by a fit to the present asymmetry data. Results for 2Δ from the ROT effect, $D \times 10^3$ from the TRI effect, the (J,K) assignments of transition states, and the ratio of fission cross sections are summarized in Table IX.

An interesting observation for the TRI effect in Table IX summarizing the results are the signs of D being negative for ^{233}U(n,f) and ^{239}Pu(n,f) but positive for ^{235}U(n,f) and ^{241}Pu(n,f). This change of signs is readily understood by inspecting the (J,K) assessments in the last row of the table. Noting that $K = 0$ states are sterile for the TRI effect, only the transition states $J_+ = (I + 1/2)$ come into play for ^{233}U and ^{239}Pu while for ^{235}U and ^{241}Pu the transition states $J_- = (I - 1/2)$ are effective. Recall that for given neutron spin orientation the angular velocities ω_z have opposite sign for J_+ and J_-. The signs of the TRI effect D hence just follow this inversion of the sense of rotation ω_z.

VII. SOME DETAILED RESULTS

In Fig. 12 the characteristic shape of the asymmetry $A(\theta_{\mathrm{TP-LF}})$ for the ROT effect is less evident for the reaction with the target ^{233}U (top left panel). But after subtracting from the experimental asymmetries the contribution of the TRI effect not depending on angle, the remaining asymmetry

TABLE IV. TRI (J,K) analysis of D for ^{233}U(n,f).

Target spin parity $I = 5/2^+-$; $\frac{\sigma_f(J_+=3)}{\sigma_f(J_-=2)} = 1.27$			
(J_+,K_+) \ (J_-,K_-)	(2,0)	(2,1)	(2,2)
(3,0)	0.0	0.86	0.69
(3,1)	−2.4	−1.5	−1.7
(3,2)	**−3.5**	−2.6	−2.8
(3,3)	−2.0	−1.1	−1.3

TABLE V. ROT (J,K) analysis of 2Δ for ^{239}Pu(n,f).

Target spin parity $I = 1/2^+$; $\frac{\sigma_f(J_+=1)}{\sigma_f(J_-=0)} = 0.48$	
(J_+,K_+) \ (J_-,K_-)	(0,0)
(1,0)	0.057
(1,1)	**0.028**

reveals the characteristic features of sign change attributed to the "pure" ROT effect. This is on display in Fig. 13 for data obtained in a control experiment with higher statistics.

For the reaction ^{235}U(n,f) the statistics of accumulated events allowed one to make more detailed tests of the ROT model. The experimental data for the asymmetries $A(\theta_{\mathrm{TP-LF}})$ were sorted into bins of the kinetic energy E_{TP} of the TPs, and then fitted by Eq. (14) for each individual E_{TP} bin. It allows determining the parameters 2Δ and D for the ROT and the TRI effect, respectively, in each E_{TP} bin. The widths of the bins were 3 MeV. As an example the asymmetries for the two TP energies $E_{\mathrm{TP}} = 12.5 \pm 1.5$ MeV and $E_{\mathrm{TP}} = 24.5 \pm 1.5$ MeV are on display in Fig. 14 as a function of the angle $\theta_{\mathrm{TP-LF}}$ together with the model fits. The experimental asymmetries $A(\theta_{\mathrm{TP-LF}})$ drawn as blue points differ widely for these two energies. The same observation is made for the angular distribution of the TPs shown as histograms becoming much wider at the higher energy. According to Eq. (9) the shape of the angular distribution enters the formula for the A_{ROT} asymmetry. Based on these experimental shapes the fit to the experimental asymmetry data becomes excellent as visualized by the red squares.

The validity of the trajectory calculations for the ROT model may be further probed by inspecting the ROT effect parameter 2Δ as a function of the kinetic energy of the TPs evaluated as described in connection with Fig. 14. The reaction considered is ^{235}U(n,f). The theoretical angular shifts 2Δ of the ROT effect are plotted in Fig. 15 as red squares while the experimental shifts are given as blue points. Except for the smallest TP energies the agreement between theory and experiment is very satisfactory. The angular shift concordantly increases across the energy spectrum shown as histogram but saturates at the highest energies. The agreement gives added confidence to the soundness of the trajectory-based ROT model. The discrepancy at small TP energy is understood to be from the missing particle identification which was not available for the experiment at hand. Hence He and H isotopes are registered as TPs. The yield of H isotopes (mostly tritons)

TABLE VI. TRI (J,K) analysis of D for ^{239}Pu(n,f).

Target spin parity $I = 1/2^+$; $\frac{\sigma_f(J_+=1)}{\sigma_f(J_-=0)} = 0.48$	
(J_+,K_+) \ (J_-,K_-)	(0,0)
(1,0)	0.0
(1,1)	**−0.38**

TABLE VII. ROT (J,K) analysis of 2Δ for ^{241}Pu(n,f).

Target spin parity $I = 5/2^+$; $\frac{\sigma_f(J_+=3)}{\sigma_f(J_-=2)} = 0.64$			
(J_+,K_+) \ (J_-,K_-)	(2,0)	(2,1)	(2,2)
(3,0)	0.030	**0.048**	0.101
(3,1)	0.019	0.036	0.090
(3,2)	−0.015	0.002	0.056
(3,3)	−0.072	−0.055	−0.001

is about 8% of the He isotopes (mostly alfas). Ternary tritons have on average smaller energies of 8.4(2) MeV compared to α particles with average energies 15.9(2) MeV. The bulge seen in experiment at low energies of the TP spectrum in Fig. 15 is therefore attributed to the contribution by tritons. Because Coulomb forces exerted by fragments on tritons are smaller than for alfas the lag angle Δ in Fig. 7 will be larger for tritons than for alfas. In the overlap region near kinetic energies of 10 MeV the effective angular shift 2Δ observed in experiment (blue points) is hence anticipated to be larger than the model shift 2Δ (red squares) calculated for α particles. This is indeed observed in Fig. 15.

It is interesting to compare the dependence on TP energy of the angular shift 2Δ for the ROT effect in Fig. 15 and the asymmetry D for the TRI effect. The TRI effects for the two reactions ^{233}U(n,f) and ^{235}U(n,f) are chosen for this comparison with the ROT effect for ^{235}U(n,f). As already pointed out, in Table IX the TRI asymmetry D is negative for ^{233}U while for ^{235}U the asymmetry is positive. For a more convenient discussion in Fig. 16 therefore the absolute value $|D|$ is shown for the ^{233}U(n,f) reaction (left panel) and D for the ^{235}U(n,f) (right panel). Catching the eye the energy spectra of TPs in the two reactions look very different. But this is simply because of the TP identification which was only operational for the ^{233}U(n,f) reaction. The spectrum shown is for α particles. Without TP identification as in the reaction ^{235}U(n,f), the spectra of tritons and α particles are superimposed leading to a broader energy distribution as discussed above.

The asymmetries in Fig. 16 are seen to increase continuously across the TP energy spectrum. This is quite different from the behavior of the ROT effect in Fig. 15. For discussion it is recalled that in the frame of the model suggested for the TRI effect it is the Coriolis force which is steering the asymmetries of TPs. The Coriolis force is proportional to the velocity of the TP at scission. In Fig. 16 the increase of the TRI effect

TABLE VIII. TRI (J,K) analysis of D for ^{241}Pu(n,f).

Target spin parity $I = 5/2^+$; $\frac{\sigma_f(J_+=3)}{\sigma_f(J_-=2)} = 0.64$			
(J_+,K_+) \ (J_-,K_-)	(2,0)	(2,1)	(2,2)
(3,0)	0.0	**1.2**	1.0
(3,1)	−1.7	−0.5	−0.7
(3,2)	−2.4	−1.2	−1.5
(3,3)	−1.4	−0.2	−0.4

TABLE IX. Summary of results.

Target	^{233}U	^{235}U	^{239}Pu	^{241}Pu
spin parity	$5/2^+$	$7/2^-$	$1/2^+$	$5/2^-$
σ_{f+}/σ_{f-}	1.27	1.76	0.48	0.64
ROT 2Δ	0.021(4)°	0.215(5)°	0.020(3)°	0.047(4)°
TRI D · 10^3	−3.90(12)	1.7(2)	−0.23(9)	1.30(15)
(J_+,K_+)	(3,2)	(4,0)	(1,1)	(3,0)
(J_-,K_-)	(2,0)	(3,2)	(0,0)	(2,1)

as a function of the experimental final TP energy appears to suggest that there is a positive correlation between TP energies at scission and in the final state. With this correlation the increase of the Coriolis force with increase of v_{TP} at scission leads to an increase of the TRI effect with the final TP energy. This correlation could not be studied in former ternary fission experiments.

As to the TRI asymmetry as a function of fragment mass for ^{233}U(n,f) in Fig. 17, it appears that the effect does not depend on mass except for a depression near mass 132 u. But this indication should be confirmed in an experiment with higher statistical accuracy.

For the reaction ^{233}U(n,f) a particular analysis was devoted to the question whether the pronounced TRI effect depends on the specific type of the ternary particle. Particle identification inferred from the silicon detector signals allowed one to separately assess the TRI asymmetry D for He and H isotopes. In ternary fission the yield of H isotopes represents less than 10% of the He isotopes. For He isotopes (mostly ^{4}He) the TRI effect was found to be $D = -3.90(12) \times 10^{-3}$, while for H isotopes (mostly ^{3}H) it is $D = -2.9(5) \times 10^{-3}$. Within error bars of 2σ the asymmetries are not significantly different. It is hence concluded that the TRI effect depends only weakly if at all on the type of the TP being emitted.

A further study addressed the question whether p-wave resonances in the compound nucleus following neutron capture are playing a role. Their impact on PNC effects is well

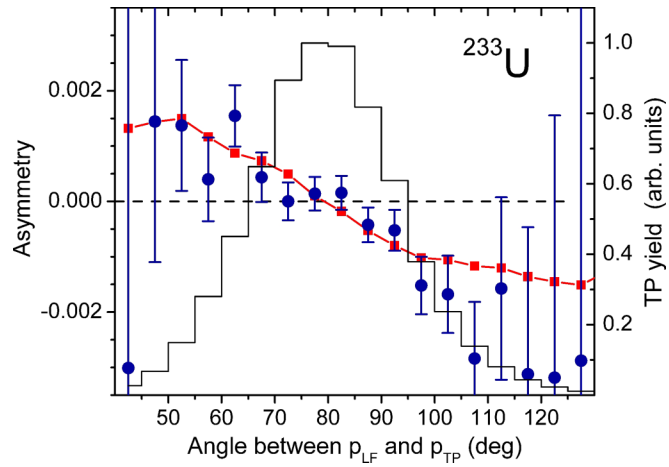

FIG. 13. Reaction ^{233}U(n,f). Experimental asymmetry after subtracting from the measured $A(\theta_{TP-LF})$ the constant $A_{TRI} = D$ (blue points). Model fit for the "pure" ROT effect (red squares). Angular distribution of TPs (histogram with scale to the right).

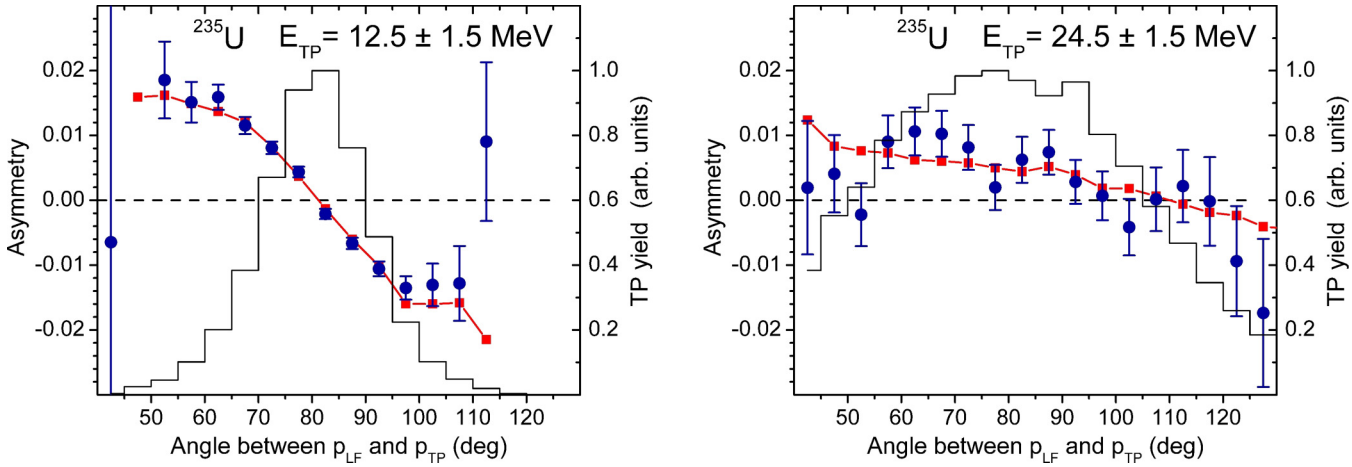

FIG. 14. ROT asymmetry $A_{\mathrm{ROT}}(\theta_{\mathrm{TP-LF}})$ in $^{235}\mathrm{U}(n,f)$ for kinetic TP energies sorted into bins with width 3 MeV at 12.5 MeV (left panel) and 24.5 MeV (right panel). Experimental data (blue points with error bars). Model fit (red squares). Angular distributions of TPs (histogram with scale to the right).

known [27]. For $^{233}\mathrm{U}(n,f)$ a strong p-wave resonance was reported to be present near the incoming neutron energy $E_n \approx 0.2$ eV where the PNC asymmetry is changing sign. At the Institut Laue-Langevin a polarized neutron beam with energy $E_n = 0.16$ eV is provided at the instrument D3 [12]. A ternary fission experiment with polarized neutrons was therefore run on this beam. The TRI asymmetry found was $D = -2.4(8) \times 10^{-3}$ and thus within error bars of 2σ compatible with $D = -3.90(12) \times 10^{-3}$ measured with cold neutrons. Hence, if interferences between nearby compound states are to play a role for the outcome of TRI effects, only neighboring s states could be concerned.

VIII. QUANTUM-MECHANICAL THEORIES PROPOSED FOR THE ROT AND TRI EFFECTS

The present experiments on ternary fission of actinides induced by polarized neutrons are unique. There are no similar experiments to compare with. On the other hand several theories have been elaborated discussing TRI and ROT effects. A purely quantum—mechanical theory studied in a first approach the TRI effect discovered in $^{233}\mathrm{U}(n,f)$ [17]. The theory is based on the correlator B of Eq. (1) which for ternary fission, however, is not derived from first principles. As a basic assumption the compound nucleus is taken to be rotating with especially the decisive role played by the Coriolis interaction being emphasized. In the theory special attention is given to the role played by interferences of s-wave resonances which for the time being are not predictable.

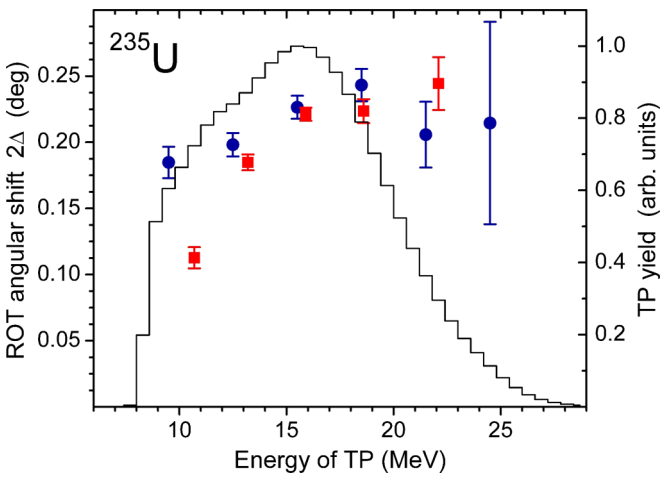

FIG. 15. Angular ROT shift 2Δ as a function of TP energy for reaction $^{235}\mathrm{U}(n,f)$. Experimental data (blue points). Theoretical calculation with TPs assumed to be α particles (red squares). The experimental TP energy spectrum is given as histogram with scale to the right.

There is a basic difference between this theory and the semiclassical TRI model expounded in Sec. V. In this latter model the notion of transition states with their characteristic collective K-quantum numbers is put at the center of discussion. Collective states with nonzero K values presuppose nuclei being not axially symmetric. In the quantum-mechanical theory, however, the nucleus is assumed to be axially symmetric and hence the K-quantum numbers cannot be collective.

A further comment concerns the angular dependence of the TRI asymmetry A_{TRI}. With the correlator B from Eq. (1) the angular dependence stipulated is $A_{\mathrm{TRI}} \sim \sin(\theta_{\mathrm{TP-LF}})$ with $\theta_{\mathrm{TP-LF}}$ the angle between the momenta $\mathbf{p}_{\mathrm{TP}}$ and $\mathbf{p}_{\mathrm{LF}}$. The range of angles $\theta_{\mathrm{TP-LF}}$ accessible to experiment is fixed by the layout of detectors in Fig. 1. In the albeit limited range $\pm 30^\circ$ around the peak of the angular TP distributions being explored there is no clear evidence for an angular dependence. However, large error bars do not allow proving firmly that there is no angular dependence at all. Anyhow, as shown in Fig. 12 a perfect fit to the asymmetry data is achieved with the TRI asymmetry A_{TRI} taken to be constant $A_{\mathrm{TRI}} = D$.

The ROT effect in $^{235}\mathrm{U}(n,f)$ being discovered later than the TRI effect instigated a generalization of the quantum-mechanical theory [28]. The idea of a rotating system was maintained with the role played by the Coriolis force being emphasized. For the ROT effect a further factor $(\mathbf{p}_{\mathrm{TP}} \cdot \mathbf{p}_{\mathrm{LF}})$ to the correlator B of Eq. (1) was inserted. The triple correlation for TRI thus becomes a quintuple correlation for ROT.

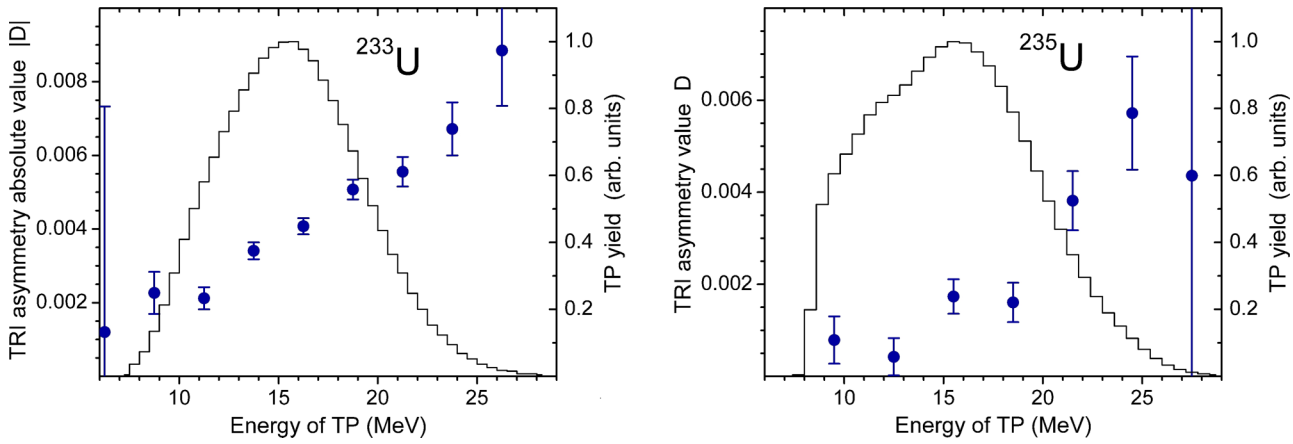

FIG. 16. TRI asymmetry as a function of TP energy (blue point with error bars). To the left $|D|$ from reaction ^{233}U(n,f), to the right D from reaction ^{235}U(n,f). (D is negative for ^{233}U and positive for ^{235}U, but for a more convenient discussion the absolute value of D is plotted for ^{233}U.) Histograms are TP energy spectra with scale to the right.

The angular dependence of the ROT asymmetry $A_{\mathrm{ROT}}(\theta_{\mathrm{TP-LF}})$ in the approach of a quintuple correlation as indicated above is $\sin(\theta_{\mathrm{TP-LF}}) \cdot \cos(\theta_{\mathrm{TP-LF}}) = \frac{1}{2}\sin(2\theta_{\mathrm{TP-LF}})$. It reproduces correctly the change of sign of A_{ROT} for angles smaller and larger than the average angle $\theta_{\mathrm{TP-LF}} = 90^\circ$ in symmetric fission. But it is at variance with the shape of the experimental asymmetry $A(\theta_{\mathrm{TP-LF}})$ as a function of angle. The variation of the asymmetry A_{ROT} with angle $\theta_{\mathrm{TP-LF}}$ in Fig. 12 is in experiment obviously a function of the slope $Y'(\theta_{\mathrm{TP-LF}})$ of the ternary particle yield $Y(\theta_{\mathrm{TP-LF}})$. In the semiclassical model discussed here all asymmetries were successfully parametrized by exploiting this dependence on slope. A slope dependence was later also adopted in a refinement of the quantum theory [29]. Yet a major difference between the quantum-mechanical and the semiclassical approach remains. While in the former case the changes of size and sign from isotope to isotope are traced to phase relations between interfering s-wave resonances, in the latter model the properties of physically measurable (J,K) transition states are considered to be decisive.

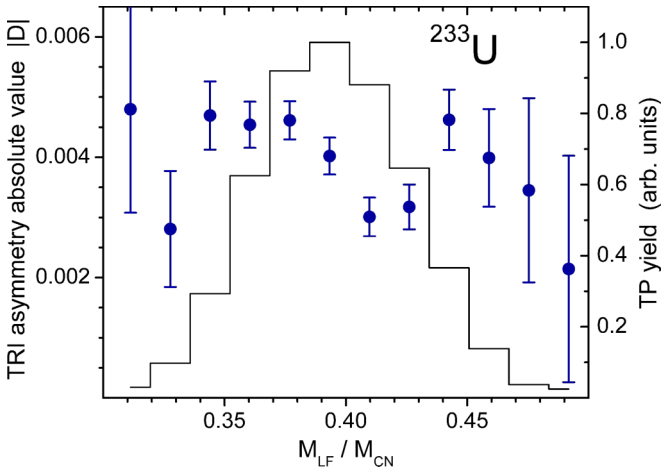

FIG. 17. Absolute value $|D|$ of TRI asymmetry as a function of ratio of light fragment mass to the mass of compound nucleus for reaction ^{233}U(n,f) (blue points with error bars). Histogram is light fragment mass distribution with scale to the right.

Recently a new idea came up for a semiclassical interpretation of TRI effects without recourse to Coriolis forces [30]. An empirical formula for the yield of ternary particles is advocated depending on the energy costs to liberate the TP. In the rotating system following capture of polarized neutrons the energy of ternary particles is a function of their angular momentum $\mathbf{l}$ and the angular velocity $\boldsymbol{\omega}$ of the rotating system. In the rotating system their energy is $E = E_0 - \boldsymbol{\omega} \cdot \mathbf{l}$ with E_0 the TP energy in the nonrotating nucleus. However, in contrast to experiment, for all four reactions having been investigated the signs of A_{TRI} anticipated are always negative. The sign switches for the TRI effect in Table IX are manifest in experiment and cannot be considered to be incidental. There is no obvious way to solve within the frame of the model this flaw.

A very different approach was suggested invoking a spin-orbit coupling between the spin of the polarized nucleus and the orbital momentum of the TP [31,32]. Together with spin the nucleus carries a magnetic moment generating a magnetic field. According to classic electrodynamics the TP experiences in this field a Lorentz force pushing it sideways. Quantitatively this force is by far too small. It is therefore speculated that a much larger nuclear spin-orbit interaction comes into play. The nature of this interaction is not discussed. Anyhow, no results are given that could be confronted to experiment.

IX. DISCUSSION

The K transition states determined in the present work for ternary fission should be compared to the transition states found in binary fission. The fission reaction for which the comparison is possible is ^{235}U(n,f). There was a longstanding effort to pin down in the neutron resonance region the K values for the two spin states $J_+ = 4^-$ and $J_- = 3^-$ of the compound transition states found in binary fission. In the most ambitious experiments a polarized neutron beam was inducing fission in a polarized ^{235}U target [1,2]. More recent experiments on binary fission in the resonance region studied angular anisotropies of fragments for oriented nuclei irradiated by un-polarized

neutrons [25]. For cold neutrons with $E_n = 4$ meV the $J_+ = 4^-$ state receives contributions (J_+, K_+) of 70% for (4,2) and of 30% for (4,1). For the $J_- = 3^-$ state the contributions to (J_-, K_-) are 70% for (3,0) and 30% for (3,1). These results from a multichannel, multilevel fit are more detailed than the data from the present experiment where per level only one channel was assumed to be effective. Nevertheless there is apparently no agreement with the assessment of states (4,0) and (3,2) determined in the present analysis of ternary fission. These findings are annoying, because from PNC studies where fragments from both binary and ternary fission exhibit the same PNC asymmetries, it was concluded that these two modes bifurcate at scission only. Instead the present discrepancies in the K assessments in binary and ternary fission give the impression that the two modes may already at the saddle point proceed along different transition states. Yet, in view of ambiguities in the assessment of K values in the neutron resonance region it should be interesting to test whether the K values found in the present experiment for ternary fission can give acceptable results for the angular anisotropies found in binary fission near the thermal point.

Thereby a particularity should be noted for the reaction ^{239}Pu(n,f). The ^{239}Pu target has the spin $I = 1/2$ which by cold neutron capture generates the compound spins $J_+ = 1$ and $J_- = 0$. Only the J_+ state can be the source of ROT and TRI effects. The transition state analysis yields unequivocally $(J_+, K_+) = (1,1)$ as the dominant transition state for J_+. But recall that the ratio of spin-dependent fission cross sections is $\sigma_f(1^+)/\sigma_f(0^+) = 0.48$ [25]. The state $(J_-, K_-) = (0,0)$ is hence present though not detected with the technique employed. The signs of the TRI and ROT effect for ^{239}Pu(n,f) follow unambiguously from the fact that only J_+ states are effective. Our model predicts the D asymmetry to be negative, similarly to the reaction ^{233}U(n,f). Indeed, for the reaction with the ^{239}Pu target $D = -0.23(9) \times 10^{-3}$. As regards the ROT effect, for the transition state $(J_+, K_+) = (1,1)$ the angular shift 2Δ is expected to be albeit small but positive. With $2\Delta = +0.020(3)^\circ$ this is what is observed.

A comment concerning the reaction ^{235}U(n,f) draws attention to the cross sections favoring J_+ (see Table IX) and the assignment of the state $(J_+, K_+) = (4,0)$ by the analysis of the ROT effect. With $K = 0$ the component R of collective rotation perpendicular to the fission axis is maximal and the corresponding angular shift $2\Delta = +0.215(5)^\circ$ is in fact the largest among the reactions studied. Because this orbital revolution of fission fragments will not contribute to their intrinsic angular momenta it makes understandable why the fragment momenta from the reactions ^{252}Cf(sf) with spin $J = 0\hbar$ are measured to be the same as in ^{235}U(n,f) with spin $J = 4\hbar$ [33]. The equality of fragment angular momenta in these two reactions was conjectured to follow from the initial compound spin of the excited ^{236}U* being hidden in collective rotation not showing up in the fragments [33]. This conjecture is proven by the present results to be valid.

For the reaction ^{241}Pu(n,f) the ratio of spin separated fission cross sections $\sigma_f(J_+)/\sigma_f(J_-)$ had to be determined in the present experiments as an additional fit parameter. The ratio found is given in Tables VII and VIII. It is at variance to a ratio communicated to us based on the analysis of neutron resonance parameters from ENDF/B-VII [26]. It should be kept in mind, however, that in this analysis above all the parameters of resonances at negative energies are delicate to assign. The discrepancies could be removed by different assignments of subbarrier resonances.

The discovery of ROT and TRI effects in fission with charged ternary particles has initiated the search for ROT and TRI effects in binary fission accompanied by neutrons and/or gammas [34,35]. The initial idea was that these effects could possibly disclose the emission of neutrons and/or gammas right at scission when the neck joining the two fragments is breaking apart. However, most neutrons and gammas are emitted by fully accelerated fragments. In fact, it appears that the ROT effect discovered in the two binary fission reactions ^{233}U(n,f) and ^{235}U(n,f) is sensing neutrons and gammas emitted by the fragments. For the TRI effect only upper limits for neutrons and gammas could be determined.

X. SUMMARY

Studies of ternary fission induced by polarized neutrons were initiated by the suggestion that similar to experiments in the decay of free polarized neutrons time reversal invariance could be explored. It was proposed that a correlation $B = \boldsymbol{\sigma}_n \cdot (\mathbf{p}_{\rm LF} \times \mathbf{p}_{\rm TP})$ between neutron spin $\boldsymbol{\sigma}_n$, the momenta $\mathbf{p}_{\rm LF}$ of light fission fragment, and ternary particles TP $\mathbf{p}_{\rm TP}$ should be analyzed. For ternary fission this correlation is not derivable from first principles and hence pure speculation. Nevertheless, experiments were first performed for the fissile isotopes ^{233,235}U, to be extended later to ^{239,241}Pu. The correlation put forth was not found. Instead two types of asymmetries in the emission of ternary particles were discovered, one is dominant for ^{233}U while a different one prevails for ^{235}U.

As shown in Fig. 1, in experiment a slow neutron beam running in the $+z$ direction and with polarization chosen to be longitudinal was hitting thin targets of the above isotopes. Detectors for fission fragments and ternary particles (mostly α particles) were mounted in a plane perpendicular to the beam. The beam polarization was flipped at a frequency near 1 Hz. In the evaluation of TP-LF coincidences the asymmetry $A \sim (N_\uparrow - N_\downarrow)$ in the count rates $N_\uparrow$ and $N_\downarrow$ for neutron spin in or against beam direction, respectively, was determined according to Eq. (3).

Near the barrier the transition states are described by the wave functions of spinning tops $D_{\rm JMK}$. The good quantum numbers are the angular momentum J, its projections M on a space-fixed z axis, and K on the axis of deformation. Semiclassically the angular momentum $\mathbf{J}$ is decomposed into the component $\mathbf{K}$ parallel to the fission axis (axis of deformation) and the component $\mathbf{R}$ perpendicular to this axis. In slow neutron induced fission the nucleus near the barrier is cold and hence $\mathbf{K}$ and $\mathbf{R}$ are necessarily collective rotations. The present experiments enabled one to determine for each nucleus studied the dominant transition states (J, K).

Following capture of longitudinally polarized neutrons the nuclei are partly polarized in the z direction: $\langle J_z \rangle \neq 0$. This means that the fissioning compound is rotating with angular velocity $\omega_z \sim \langle J_z \rangle$ around the neutron beam axis. In the breakdown of the angular momentum $\mathbf{J}$ into its components

K and **R** the relative weights given to them depends on the structure of the fissioning nucleus. For the interpretation of results semiclassical models are proposed.

A first model explores the consequences of collective rotations of the fissioning system around an axis pointing perpendicular to the fission axis (see Fig. 7). It is shown that upon flipping neutron spin the angular distributions of TPs are wobbling back and forth by the angle Δ as visualized in Fig. 5. In the slopes of the two shifted angular TP distributions an asymmetry $A \sim (N_\uparrow - N_\downarrow)$ shows up depending on the angle $\theta_{\mathrm{TP-LF}}$ between the momenta of TP and LF. It is changing sign for angles smaller or larger than the peak angle $\theta \approx 82^\circ$ of TP angular distributions. At the peak angle $A = 0$. This is in fact observed in experiment (see Fig. 3). The effect is called the ROT effect.

For a quantitative assessment of the ROT effect trajectory calculations were performed for all possible (J,K) combinations. Sizes and signs of the ROT effect are thus specified in terms of transition states (J,K). It is confirmed that the effect is best pronounced for $K = 0$ and thus maximal **R** as anticipated intuitively. It has to be underlined that the model reproduces quantitatively the experimental findings.

A further asymmetry refers to TP emission yields relative to a plane spanned in Fig. 1 by the axis of neutron polarization ($+z$ direction) and the LF momentum ($+x$ direction). This plane defines two hemispheres, in Fig. 1 an upper and a lower one. Depending on neutron spin orientation $\sigma_z = \pm\frac{1}{2}\hbar$ and capture state $J_\pm = (I \pm 1/2)$ the emission of TPs in a given hemisphere is either favored or hindered. The model proposed attributes the effect to a rotation of the fission prone nucleus around the fission axis with a nonzero $K \neq 0$. A collective nonzero K requires, however, breaking the axial symmetry of the fissioning nucleus. Broken axial symmetry is known from bending modes excited near scission. For the present discussion the two degenerate bending vibrations at right angles relative to each other are viewed as two rotations of a bent nucleus with opposite senses of rotation. Loosely speaking the modes are resembling rotating bananas. Unavoidably there is even for maximum $K = J$ still a component ω_z around the axis of nuclear polarization. Turning to ternary fission, the TPs to be ejected from the neck joining the two main fragments are located between the tips of the rotating fragments and participate in the rotation thereby moving up and down in the y direction. As visualized in Fig. 11 they will hence experience a Coriolis force acting along the fission axis in the x direction. In theoretical models the TPs are released from the light fragment [24]. Depending on the sense of rotation, TP ejection is either favored or hindered. With this approach the signs for the asymmetries are correctly predicted for all reactions studied. The detailed analysis of this effect called the TRI effect allows like for the ROT effect the assessment of (J,K) transition states. The two effects yield concordant results. The (J,K) states obtained in the analysis of the ROT effect predict correctly the signs of the TRI asymmetry with only one calibration constant required for the size of the TRI effect adopted from the reaction $^{235}\mathrm{U}(n,f)$ for all other reactions studied.

In a graphic summary of results on display in Fig. 18, a zoom of asymmetries near the peak angle of the angular TP distribution is visualized for all four reactions investigated. In all reactions both effects, ROT and TRI, contribute though with different weights. The two effects are readily disentangled in the figure. It is exploited that, in a plot of the asymmetry $A(\theta_{\mathrm{TP-LF}})$ as a function of the angle $\theta_{\mathrm{TP-LF}}$ between the trajectories of TP and LF, the ROT effect is nil at the peak angle $\theta_{\mathrm{TP-LF}} \approx 82^\circ$ of the angular distribution. At this angle only the constant TRI effect not depending on angle is responsible for the asymmetry observed. The constant TRI asymmetry $A_{\mathrm{TRI}} = D$ is marked by dots at this angle. The TRI asymmetry has both positive and negative signs. It is largest in absolute size for the reaction $^{233}\mathrm{U}(n,f)$. The sloping curves depict the ROT asymmetries as a function of angle $\theta_{\mathrm{TP-LF}}$. Relative to the TRI asymmetry the ROT asymmetry changes sign at the peak angle $\theta_{\mathrm{TP-LF}}$. The steepness of the slope as a function of the angle $\theta_{\mathrm{TP-LF}}$ is a measure for the lag angle Δ in the turning around of the LF and TP trajectories in fission induced by polarized neutrons. It is largest for the reaction $^{235}\mathrm{U}(n,f)$.

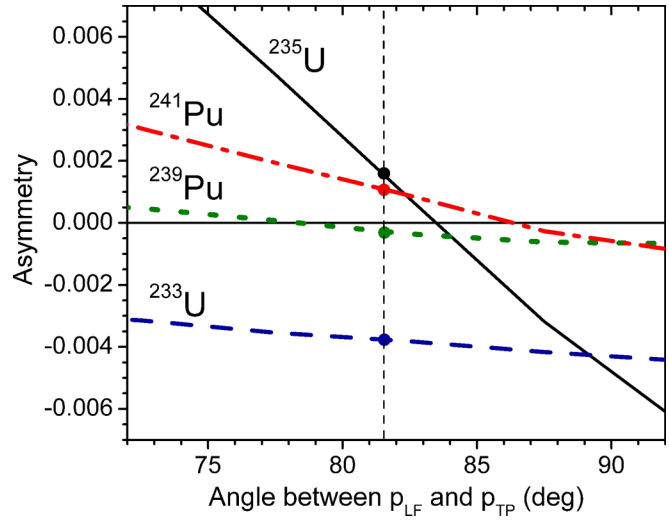

FIG. 18. Zoom of asymmetries $A(\theta_{\mathrm{TP-LF}})$ near the peak angle $\theta_{\mathrm{TP-LF}} \approx 82^\circ$ of angular TP distributions.

Somewhat unexpectedly the study of asymmetries of TP emission in ternary fission induced by slow polarized neutrons has proven to be a novel method for the spectroscopy of transition states (J,K) near the fission barrier.

It is worth noting that the present assignments of (J,K) states in ternary fission are at variance with the assignments in binary fission from the literature. However, these latter assignments are not unambiguous and it would be interesting to see whether the present results could also for binary fission be a valid description.

ACKNOWLEDGMENTS

Thanks for their competent support are due to the reactor and instrument divisions of the Institut Laue-Langevin. The contribution of the detector laboratory and the electronic workshop from the Institute of Nuclear Physics of Darmstadt Technical University is highly appreciated. Grants provided by the RFBR (Russian Federation) and the DFG (Germany) are gratefully acknowledged.

[1] R. I. Schermer, L. Passell, G. Brunhart, C. A. Reynolds, L. V. Sailor, and F. J. Shore, Phys. Rev. **167**, 1121 (1968).

[2] M. S. Moore, J. D. Moses, G. A. Keyworth, J. W. T. Dabbs, and N. W. Hill, Phys. Rev. C **18**, 1328 (1978).

[3] G. V. Danilyan, B. D. Vodennikov, V. P. Dronyaev, V. V. Novitsky, V. S. Pavlov, and S. P. Borovlyev, JETP Lett. **26**, 186 (1977).

[4] A. Belozerov, A. G. Beda, S. I. Burov, G. V. Danilyan, A. N. Martem'yanov, V. S. Pavlov, V. A. Shchenev, L. N. Bondarenko, Yu. A. Mostovoi, G. Geltenbort, I. Last, K. Schrekenbach, and F. Gönnenwein, JETP Lett. **54**, 132 (1991).

[5] F. Gönnenwein, A. V. Belozerov, A. G. Beda, S. I. Burov, G. V. Danilyan, A. N. Martem'yanov, V. S. Pavlov, V. A. Shchenev, L. N. Bondarenko, Yu. A. Mostovoi, P. Geltenbort, J. Last, and K. Schreckenbach, Nucl. Phys. A **567**, 303 (1994).

[6] P. Jesinger, A. Kötzle, F. Gönnenwein, M. Mutterer, J. von Kalben, G. V. Danilyan, V. S. Pavlov, G. A. Petrov, A. M. Gagarski, W. H. Trzaska, S. M. Soloviev, V. V. Nesvizhevski, and O. Zimmer, Phys. At. Nucl. **65**, 630 (2002).

[7] K. Schreckenbach, J. van Klinken, and J. Last, in *Time Reversal Invariance and Parity Violation in Neutron Reactions: Proceedings of the 2nd International Workshop, Dubna, Russia, May 4–7, 1993*, edited by C. R. Gould, J. D. Bowman, and Y. P. Popov (World Scientific Publishing Company, Singapore, 1994), p. 187.

[8] P. Jesinger, A. Kötzle, A. Gagarski, F. Gönnenwein, G. Danilyan, V. Pavlov, V. Chvatchkin, M. Mutterer, S. Neumaier, G. Petrov, V. Petrova, V. Nesvizhevsky, O. Zimmer, P. Geltenbort, K. Schmidt, and K. Korobkina, Nucl. Instrum. Methods Phys. Res. A **440**, 618 (2000).

[9] F. Gönnenwein, M. Mutterer, A. Gagarski, I. Guseva, G. Petrov, V. Sokolov, T. Zavarukhina, Y. Gusev, J. von Kalben, V. Nesvizhevski, and T. Soldner, Phys. Lett. B **652**, 13 (2007).

[10] H. Abele, D. Dubbers, H. Häse, M. Klein, A. Knöpfler, M.Kreuz, T. Lauer, B. Märkisch, D. Mund, V. Nesvizhevsky, A. Petoukhov, C. Schmidt, M. Schumann, and T. Soldner, Nucl. Instrum. Methods Phys. Res. A **562**, 407 (2006).

[11] G. Cicognani, editor, in *The Yellow Book, Guide to Neutron Research Facilities* (Insitut Laue-Langevin, Grenoble, 2008), p. 110.

[12] G. Cicognani, editor, in *The Yellow Book, Guide to Neutron Research Facilities* (Insitut Laue-Langevin, Grenoble, 2008), p. 34.

[13] M. Mutterer, W. H. Trzaska, G. P. Tyurin, A. V. Evsenin, J. von Kalben, J. Kemmer, M. Kapusta, V. G. Lyapin, and S. V. Khlebnikov, IEEE Trans. Nucl. Sci. **47**, 756 (2000).

[14] A. Gagarski, I. Guseva, F. Gönnenwein, G. Petrov, P. Jesinger, V. Sokolov, T. Zavarukhina, M. Mutterer, J. von Kalben, W. Trzaska, S. Khlebnikov, G. Tiourine, S. Soloviev, V. Nesvizhevsky, O. Zimmer, and T. Soldner, in *Neutron Spectroscopy, Nuclear Structure, Related Topics: Proceedings of the XIV International Seminar on Interaction of Neutrons with Nuclei, Dubna, May 24–27, 2006* (Joint Institute for Nuclear Research, Dubna, Russia, 2007), p. 93.

[15] A. Bohr, in *Proceedings of the International Conference on the Peaceful Uses of Atomic Energy, Geneva, August, 1955*, Vol. 2 (United Nations Publication, New York, 1956), p. 151.

[16] R. Vandenbosch and J. R. Huizenga, *Nuclear Fission* (Academic Press, New York, 1973).

[17] V. E. Bunakov and S. G. Kadmensky, Phys. At. Nucl. **66**, 1846 (2003).

[18] I. S. Guseva and Yu. I. Gusev, Bull. Russ. Acad. Sci., Phys. Ser. **71**, 367 (2007).

[19] I. Guseva and Yu. Gusev, AIP Conf. Proc. **1175**, 355 (2009).

[20] V. E. Bunakov and S. G. Kadmensky, Phys. At. Nucl. **71**, 1200 (2008).

[21] J. R. Nix and W. J. Swiatecki, Nucl. Phys. **71**, 1 (1965).

[22] J. O. Rasmussen, W. Nörenberg, and H. J. Mang, Nucl. Phys. A **136**, 465 (1969).

[23] M. Zielinska-Pfabé and K. Dietrich, Phys. Lett. B **49**, 123 (1974).

[24] V. A. Rubchenya and S. G. Yavshits, Z. Phys. A **329**, 217 (1988).

[25] Yu. N. Kopatch, A. B. Popov, W. I. Furman, D. I. Tambovtsev, L. K. Kozlovsky, N. N. Gonin, and J. Kliman, in *Seminar on Fission Pont d'Oye IV, Castle of Pont d'Oye, Habay-la-Neuve, Belgium, 5–8 October, 1999*, edited by C. Wagemans, O. Serot, and P. D'hondt (World Scientific, Singapore, 2000), p. 123.

[26] V. M. Maslov, private communication, 2009; calculation based on evaluated nuclear data files ENDF/B-VI.

[27] G. A. Petrov, G. V. Valskii, A. K. Petukhov, A. Y. Alexandrovich, Yu. S. Pleva, V. E. Sokolov, A. B. Laptev, and O. A. Scherbakov, Nucl. Phys. A **502**, 297 (1989).

[28] V. E. Bunakov, S. G. Kadmensky, and S. S. Kadmensky, Phys. At. Nucl. **71**, 1887 (2008).

[29] V. E. Bunakov, S. G. Kadmensky, and S. S. Kadmensky, Phys. At. Nucl. **73**, 1429 (2010).

[30] V. E. Bunakov and S. G. Kadmensky, Phys. At. Nucl. **74**, 1655 (2011).

[31] A. L. Barabanov, in *Neutron Spectroscopy, Nuclear Structure, Related Topics: Proceedings of the IX International Seminar on Interaction of Neutrons with Nuclei, Dubna, May 23–26, 2001* (Joint Institute for Nuclear Research, Dubna, Russia, 2001), p. 93.

[32] A. L. Barabanov, Phys. Part. Nucl. Lett. **10**, 336 (2013).

[33] J. O. Rasmussen and R. Donangelo, in *Fission and Properties of Neutron-Rich Nuclei: Proceedings of the International Conference, Sanibel Island, Florida, USA, 10–15 November, 1997*, edited by J. H. Hamilton and A. V. Ramayya (World Scientific, Singapore, 1998), p. 150.

[34] G. V. Valsky, A. M. Gagarski, I. S. Guseva, D. O. Krinitsin, G. A. Petrov, Yu. S. Pleva, V. E. Sokolov, V. I. Petrova, T. A. Zavarukhina, and T. E. Kuzmina, Bull. Russ. Acad. Sci., Phys. Ser. **74**, 767 (2010).

[35] G. V. Danilyan, J. Klenke, Yu. N. Kopach, V. A. Krakhotin, V. V. Novitsky, V. S. Pavlov, and P. B. Shatalov, Phys. At. Nucl. **77**, 677 (2014).